Draft version December 13, 2022
Typeset using LaTeX **modern** style in AASTeX631

UV-driven Chemistry as a Signpost for Late-stage Planet Formation

Jenny K. Calahan,[1] Edwin A. Bergin,[1] Arthur D. Bosman,[1] Evan Rich,[1] Sean M. Andrews,[2] Jennifer B. Bergner,[3] L. Ilsedore Cleeves,[4] Viviana V. Guzmán,[5,6] Jane Huang,[1] John D. Ilee,[7] Charles J. Law,[2] Romane Le Gal,[2,8,9,10] Karin I. Öberg,[2] Richard Teague,[2,11] Catherine Walsh,[7] David J. Wilner,[2] and Ke Zhang[12]

[1] *University of Michigan, 323 West Hall, 1085 South University Avenue, Ann Arbor, MI 48109, USA*
[2] *Center for Astrophysics |Harvard & Smithsonian, 60 Garden St., Cambridge, MA 02138, USA*
[3] *University of Chicago Department of the Geophysical Sciences, Chicago, IL 60637, USA**
[4] *Department of Astronomy, University of Virginia, Charlottesville, VA 22904, USA*
[5] *Instituto de Astrofísica, Ponticia Universidad Católica de Chile, Av. Vicuña Mackenna 4860, 7820436 Macul, Santiago, Chile*
[6] *Núcleo Milenio de Formación Planetaria (NPF), Chile*
[7] *School of Physics & Astronomy, University of Leeds, Leeds LS2 9JT, UK*
[8] *IRAP, Université de Toulouse, CNRS, CNES, UT3, 31400 Toulouse, France*
[9] *IPAG, Université Grenoble Alpes, CNRS, IPAG, F-38000 Grenoble, France*
[10] *IRAM, 300 rue de la piscine, F-38406 Saint-Martin d'Hères, France*
[11] *Department of Earth, Atmospheric, and Planetary Sciences, Massachusetts Institute of Technology, Cambridge, MA 02139, USA*
[12] *Department of Astronomy, University of Wisconsin-Madison, 475 N Charter St, Madison, WI 53706*

ABSTRACT

The chemical reservoir within protoplanetary disks has a direct impact on planetary compositions and the potential for life. A long-lived carbon-and nitrogen-rich chemistry at cold temperatures (≤ 50 K) is observed within cold and evolved planet-forming disks. This is evidenced by bright emission from small organic radicals in 1–10 Myr aged systems that would otherwise have frozen out onto grains within 1 Myr. We explain how the chemistry of a planet-forming disk evolves from a cosmic-ray/X-ray-dominated regime to a ultraviolet-dominated chemical equilibrium. This,in turn, will bring about a temporal transition in the chemical reservoir from which planets will accrete. This photochemical dominated gas phase chemistry develops as dust evolves via growth, settling and drift, and the small grain population is depleted from the disk atmosphere. A higher gas-to-dust mass ratio allows for deeper penetration of ultraviolet photons is coupled with a carbon-rich gas (C/O > 1) to form carbon-bearing radicals and ions. This further results in gas phase formation of organic molecules, which then would be accreted by any actively forming planets present in the evolved disk.

MAIN

Protoplanetary disks are the natal environments for planets. Disks have three main components: a pebble-rich dusty midplane (dust grain radius $>\sim$ 1mm), a gaseous atmosphere extending well above(Miotello et al. 2022) and radially beyond (by a factor of $\sim$2(Ansdell et al. 2018)) the pebble-rich midplane, and a small dust population (radius < 10 μm) that is coupled to the gas. Each component of the protoplanetary disk has an impact on shaping the chemistry of actively forming planets. The solid cores of giant planets must form over a short timescale ($\sim$1 Myr) for the eventual planet to obtain its full mass over the course of a typical lifetime of gas in a disk (3-10 Myr(Haisch et al. 2001)) and to explain the widely observed gap and ring structures that are thought to be indicative of planet formation(Andrews et al. 2018). The compositions of pebbles and their icy mantles directly influence the final composition of a solid planetary core (Öberg et al. 2011; Johansen and Lambrechts 2017). After a core becomes sufficiently massive, planets start to accrete material from the gaseous reservoir surrounding the pebble-rich midplane of a protoplanetary disk to form their atmospheres (Lambrechts et al. 2014). It remains difficult to directly probe the gas within the planet-forming midplane due to the high dust densities leading to elevated dust optical depths that mask line emission, as well as cold temperatures which leads to the freezing out common gas tracers such as CO onto dust grains. However, constraining the chemical environment of the planet-forming midplane is essential to connect sub-mm observations probing the warm intermediate regions above the disk midplane to the composition of actively forming planets.

The molecules CH_3CN and HC_3N are two of many complex organic molecules (loosely defined as a molecules with at least four atoms, including multiple carbon atoms) that could act as basic precursors to prebiotic molecules(Powner et al. 2009; Ritson and Sutherland 2012; Sutherland 2015). CH_3CN and HC_3N have been observed and spatially resolved towards the protoplanetary disks around six young stars: GM Aur, AS 209, HD 163296, MWC 480, LkCa 15, and V4046 Sgr (Bergner et al. 2018; Ilee et al. 2021; Kastner et al. 2018; Öberg et al. 2015). CH_3CN has also been spatially resolved observed toward the TW Hya disk(Loomis et al. 2018), and a couple of small ($\approx$4 source) surveys have detected unresolved CH_3CN or HC_3N emission from other young stellar objects(Chapillon et al. 2012). These molecules exhibit bright emission signifying high gas phase abundances and column densities (N_{Total}=10^{12}-10^{13}cm^{-2} (Bergner et al. 2018; Ilee et al. 2021)). CH_3CN is an excellent probe of gas temperature due to multiple transitions tracing a range of energy states [lowest energy state E_L $\approx$5 K, spanning lower energy states over ΔE_L=$\sim$100 K] that can be observed simultaneously. Each J-transition (where J is the rotational quanum number) has a series of K-ladder transitions (where K is the quantum number of angular momentum along the molecular axis) which are only sensitive to collisions,

* NASA Hubble Fellowship Program Sagan Fellow

thus the ratio between K-transitions depends only on the gas density and temperature. The K-transitions span a large range of temperatures and are sufficiently close in frequency to observe in one spectral setting with the *Atacama Large Millimeter/submillimeter Array (ALMA)*. Analyses of rotational diagrams(Goldsmith and Langer 1999) made from CH_3CN observations demonstrate an origin in gas with a temperature between 25-50 K(Ilee et al. 2021), well below the expected desorption temperature (100-124 K(Corazzi et al. 2021)). Thus, the brightly observed flux from this species and similar nitriles and organics like HC_3N, and CH_2CN(Canta et al. 2021) present a chemical conundrum as they should not be present in the gaseous state; rather, they should be frozen on cold grain surfaces. Where CH_3CN and other carbon-rich molecules reside and how they are replenished in the gas phase has a substantial impact on our understanding of prebiotic enrichment into gaseous planet atmospheres. The traditional solution to this apparent discrepancy has been to turn to grain-surface chemistry. Simple carbon- and nitrogen-bearing molecules can undergo hydrogenation or other reactions to form complex organics on the surface of a grain that then non-thermally desorb the grain intact. This solution has been used to explain the organic inventories locked onto pebbles and icy grains (Öberg et al. 2011; Bergner and Ciesla 2021). This dust chemistry path requires both an intact photodesorption rate of CH_3CN from the grains of 10^{-3} mols/photon(Walsh et al. 2014; Loomis et al. 2018) and a reactive desorption efficiency(Vasyunin and Herbst 2013) of 1%. Laboratory experiments find an intact photodesorption efficiency of CH_3CN to be orders of magnitude less efficient (10^{-5} mols/photon(Basalgète et al. 2021)) and reactive desorption has not been well studied in laboratory experiments for these species. We posit here that there is a simpler alternative based solely on disk evolution processes that have been previously theorized and observed which link the disk gas chemistry to planet formation. This involves two ingredients: (1) an elevated C-to-O ratio in the gas and (2) greater penetration of UV photons due to a reduction in the total surface area of small grain population due to pebble formation. These combine to power a state of photo-chemistry equilibrium.

There has been mounting evidence for an elevated C-to-O gas phase ratio at large radial distances in evolved and cool gas-rich protoplanetary disks. Brighter than expected emission from small hydrocarbons such as C_2H (Miotello et al. 2019; Bosman et al. 2021a) and complex organics such as c-C_3H_2 (Cleeves et al. 2021) in disks and HC_3N and CH_3CN in photon-dominated regions(Le Gal et al. 2019) have independently suggested a C-to-O ratio well above the solar abundance ratio (C-to-O$\approx$0.55) (Asplund et al. 2021). As a radical, C_2H has a short lifetime (<1000 years), but it is found to be abundant in the gas. Bosman et al. 2021(Bosman et al. 2021a) find that the only way to reproduce the high column densities observed was to increase the C-to-O ratio throughout the full disk to between 1-2. They found that it was also necessary for C_2H to exist in high density gas while remaining above the disk midplane (height/radius$\approx$0.1-0.2) where UV photons dominate the high-energy

photon budget. Together, this produces a long-lived carbon-rich gas phase cycle in photochemical equilibrium(Bosman et al. 2021a). One critical factor is that C_2H is predicted and is observed to exist above the disk midplane(Law et al. 2021b). In contrast, CH_3CN has been observed to emit closer to the midplane(Ilee et al. 2021). Extending the carbon-rich chemical environment that is used to explain C_2H observations to the midplane could allow for gas phase formation of complex molecules in the planet-forming zone. Elevated C-to-O ratios would be necessary to supply the materials to create hydrocarbons and nitriles. However, this alone would not alleviate the issue of CH_3CN and HC_3N existing in the gas at temperatures at which they should be frozen and locked onto grains.

A non-thermal desorption mechanism is needed to increase the number of molecules that are being desorbed from the grains, either intact or as fragments of larger molecules. If the disk atmosphere is small-dust rich, with a gas-to-dust ratio close to the typical interstellar medium (ISM) mass ratio (gas-to-dust = 100) then UV radiation cannot penetrate deep into the disk. In this case, only high energy radiation (X-rays and cosmic rays) can penetrate the dust and gas and drive the chemistry within and near the midplane. Small dust grains are the main opacity source for UV photons which are readily produced by the young and active star. As the protoplanetary disk evolves, small dust grains agglomerate and eventually settle downwards and drift inward radially as they grow in size(Andrews and Birnstiel 2018; Birnstiel et al. 2012), decreasing the total surface area of the small grain population. As the main opacity source begins to deplete, UV photons can penetrate deeper into the disk. Here, complete desorption of CH_3CN or HC_3N is inhibited due to the dense and cold environment(Le Gal et al. 2019). This mechanism would have an effect on all molecules residing on grains, and a brief discussion regarding this can be found in the Supplemental Materials, in the section 'Implications on other molecules'.

The combined effect of a high C-to-O ratio and excess UV flux allows for complex molecules to exist within the gas phase at cold, midplane temperatures. Thus bright hydrocarbon and nitrile (i.e. C_2H, CH_3CN) emission from the cold midplane acts as a signpost for an evolved dust population, coincident with an advanced stage of planet formation including the accumulation of gas-giant atmospheres. The chemical scenario we put forward, comparing early and late-stage disk environments is shown in Figure 1. The disks observed in the Molecules with ALMA at Planet-forming Scales (MAPS) large program(Öberg et al. 2021) provide plausible support for this theory. The youngest disks in the MAPS sample reside around IM Lup and AS 209 which are on the order of 1-2 Myr old(Öberg et al. 2021). Towards the youngest source, IM Lup, there is no detection of CH_3CN nor HC_3N. AS 209 has detections of CH_3CN and HC_3N which suggest both molecules emit from $z/r>0.1$. The disk systems surrounding stars >6 Myr have CH_3CN detected at $z/r<0.1$ as determined by the modeled thermal structure and detected rotational temperature from the K-ladder transitions. This complex organic-rich midplane will influence the atmospheres

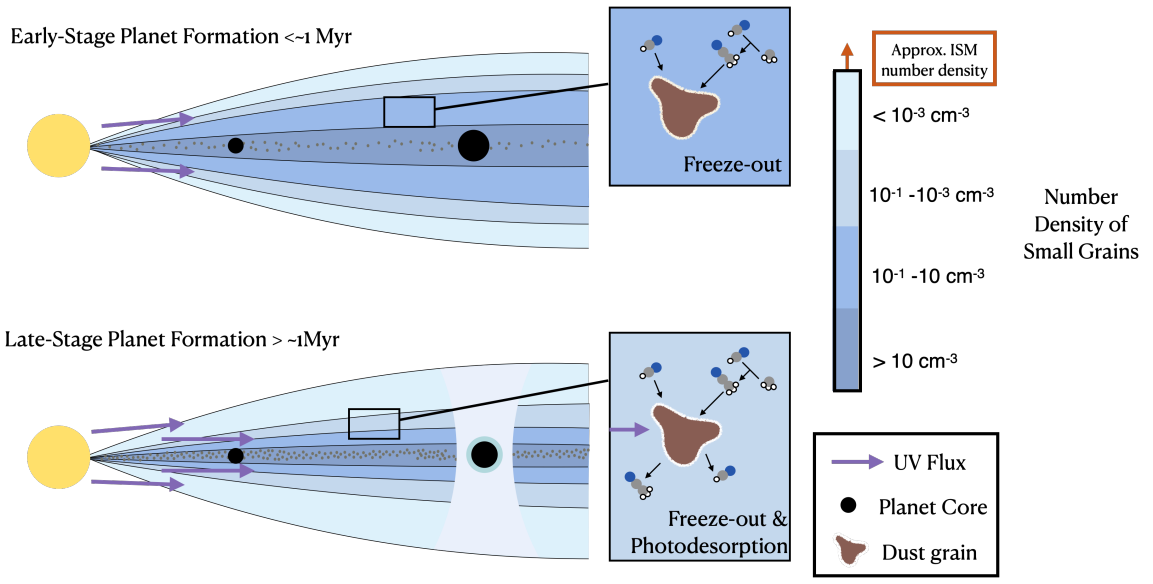

Figure 1. A schematic highlighting the physical evolution of a disk and how that physical environment can affect the chemistry. At the top, we show a disk with a large amount of small dust that acts to block UV photons. As the small dust settles, UV photons make their way deeper into the disk, allowing for photodesorption of complex species off grains. Now, there is a cycle of carbon chemistry that can be observed in the gas phase.

of planetary companions. It is worth noting that the oldest disk systems in the MAPS program exist around Herbig stars while the youngest systems are T Tauri stars. The UV-bright spectrum innate to Herbig stars may additionally influence the push of complex molecules towards the planet-forming midplane. Currently, the MAPS sample contains the bulk of the resolved CH_3CN and HC_3N data towards protoplanetary disks. To explore the effect of the stellar spectrum on CH_3CN and HC_3N emission more disks with a wide range of stellar host masses would need to be observed.

To test the validity of this proposed end-stage chemistry, we first explored single point models representative of the disk midplane with corresponding cold temperatures and high gas densities (approximately 35 K, $5{\times}10^{11}$ mol/cm^{-3}). We varied the gas-to-dust mass ratio and initial carbon abundance among other physical and chemical variables including the nitrogen abundance, dust extinction, and ionization rate. We found that the gas phase CH_3CN abundance was the most sensitive to the gas-to-dust ratio and initial gas phase carbon abundance. We then produced a thermo-chemical model representing the disk around the Herbig Ae star HD 163296. This disk is old (approx. 7.6 Myr)(Bergner et al. 2019) and is nearby at 101 pc(Gaia Collaboration et al. 2018) and has observed jets and winds (Booth et al. 2021; Xie et al. 2021). The HD 163296 disk has been widely observed in multiple gas and dust tracers with high spatial resolution (∼10 au) with clear gap and ring structures typically assumed to be associated with active planet formation(Andrews et al. 2018; Öberg et al. 2021). There is bright CH_3CN emission coming from ∼35 K gas as well

Table 1. Modeling Parameters: TW Hya & HD 163296

Parameters	**TW Hya**			**HD 163296**		
	Gas	Small Dust	Large Dust	Gas	Small Dust	Large Dust[a]
Mass ($M_\odot$)	0.025	1.0×10^{-4}	4.0×10^{-4}	0.14	2.6×10^{-5}	0.024
Ψ	1.1	1.2	1.2	1.08	1.08	1.08
γ	0.75	0.75	1.0	0.8	0.8	0.1
h_c (au)	42	42	8.4	8.44	8.44	n/a
r_c (au)	400	400	400	165	165	n/a
r_{in} (au)	0.1	0.5	1	0.45	0.45	0.45
r_{out} (au)	200	200	200	600	600	240

NOTE—Final values of the TW Hya and HD 163296 models that reproduce CO, HD, CH_3CN, HCN, and HC_3N observations when available. r_{in} and r_{out} are the radial inner and outer limits of the disk, beyond these limits there is assumed to be no gas nor dust. [a] The surface density of the large dust distribution in HD 163296 is empirically set by continuum observations, thus it is not smooth and it is not dictated by the parametric equations.

as bright emission from HC_3N and HCN(Ilee et al. 2021; Bergner et al. 2021). Our modeling efforts follow that of Zhang et al. 2021(Zhang et al. 2021), and Calahan et al. 2021b(Calahan et al. 2021b) which set up a thermo-chemical model of the HD 163296 disk by reproducing the mm dust-continuum observations, the spectral-energy distribution (SED), the full line intensity and morphology of six CO isotopologue transitions, and the vertical distribution of the optically thick lines. The model of HD 163296 started with a gas-to-small dust ratio of the disk equal to 500(Zhang et al. 2021) which was needed to reproduce the disk's SED.

RESULTS

To produce this end-stage chemical environment, we deplete the small dust mass by a factor of 10 throughout the disk of HD 163296 making the new gas-to-dust mass ratio above the pebble disk midplane equal to 5,000. We then enhanced the initial gas phase carbon abundance in the system in the form of C, CH_4, or C_2H, increasing the overall gas phase carbon-to-oxygen ratio in both disks to above unity. There are two possible sources for excess carbon in protoplanetary disks, either through the destruction of refractory carbon grains(Bosman et al. 2021b) or CO depletion through mechanisms such as reactions with ionized molecules and atoms such as He^+ or H_3^+(Schwarz et al. 2018) and a series of chemical and freeze-out processes. We note that while signatures of CO depletion are found in the HD 163296 disk(Zhang et al. 2021; Calahan et al. 2021b), CO destruction likely only occurs in environments with a high cosmic-ray flux [$2\times10^{-17}s^{-1}$](Schwarz et al. 2018). Additionally, CO destruction would supply equal amounts of carbon and oxygen, while we seek to enhance carbon over oxygen. Our

thermo-chemical model is run for a full megayear (Myr), after which the chemistry reaches an equilibrium. Notable chemical feedback due to dust evolution is predicted to occur over scales of ∼1 Myr(Krijt et al. 2018; Van Clepper et al. 2022), thus we use ∼1 Myr as an approximate length of time for the chemical environment to transition from 'early-stage' to 'late-stage' dust evolution and subsequently exist in a state of photochemical equilibrium. Gas phase chemical reactions and rates were taken from the chemical network derived in Bosman et al. 2018(Bosman et al. 2018) which in turn relies on the UMIST Database for Astrochemistry Rate12 version(McElroy et al. 2013) (see Methods section for more details). We found that regardless of the carrier of carbon, using a C/O = 1-2 and a factor of 10 depletion of small dust roughly reproduces line ratios and fluxes of the radial intensity profiles of CH_3CN, HC_3N, and HCN (see Figure 2). In this proposed scenario, ∼96% of the total mass of CH_3CN continues to reside frozen out onto grains, but the increase in UV flux allows for sufficient CH_3CN to exist and be formed in the gas to reproduce observed radial intensity profiles and column densities.

Figure 3 shows the two-dimensional number densities of CH_3CN and HC_3N. The inner ∼20 au exhibited brighter or more centrally peaked emission than was seen in observations if the C-to-O ratio = 2 throughout the full disk. To counteract this, we set the C-to-O ratio = 0.47, or the ISM ratio, inside of (∼20 au) where Zhang et al. 2021(Zhang et al. 2021) found an ISM ratio of H_2/CO (See Supplementary Figure 2). The inner disk emission remains slightly brighter than observed in HCN and CH_3CN (see Figure 2) with this alteration. This could be accounted for via a depletion in the nitrogen abundance within the N_2 ice line, a strong buildup of pebbles around the water ice line (∼5au), a lower HCN desorption energy, or a combination of these effects. Additionally, the observations may also be affected by processes such as beam smearing and a higher dust opacity than modeled. A comparison model without a depletion in small dust mass is shown in Supplementary Figure 5.

DISCUSSION

HC_3N and CH_3CN are built up in the gas from simple carbon and nitrogen-based volatiles (see Methods section "Chemical Reactions" for details). A reservoir of these more simple molecules is maintained in the gas phase due to photodesorption from dust grain surfaces by an enhanced UV-field. The main destruction products from CH_3CN and HC_3N are simple volatiles that can cycle back to create larger nitrile molecules including their original parent molecule. While there are enough complex organic molecules in the gas phase to observe bright emission, the majority of the CH_3CN, HC_3N, and HCN near the midplane still remains frozen out onto grains. The carbon-rich gas reservoir and UV-dominated disk together allow for a cycle of carbon chemistry to remain active in the gas phase. This implies that actively accreting gas giants will build their atmosphere out of this complex nitrile-enhanced material. Gas giant planets with atmospheres containing a chemical make-up with a C-to-O ratio

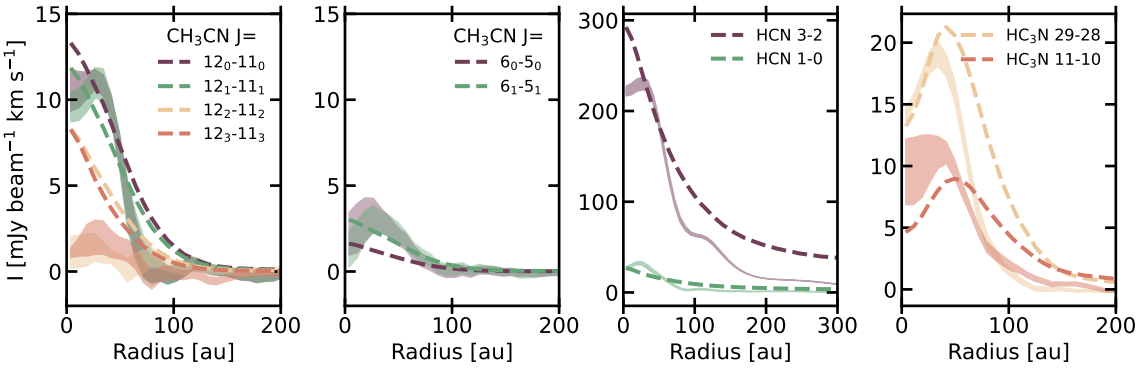

Figure 2. Radial intensity profiles of the observed complex organic molecules and HCN towards the disk around HD 163296. The molecules shown are CH_3CN, HCN, and HC_3N (left to right with two J transition of CH_3CN shown in the first two panels). Solid thick lines in the background correspond to the observations derived from Ilee et al 2021(Ilee et al. 2021) and Guzmán et al. 2021(Guzmán et al. 2021) (which utilized Law et al. 2021(Law et al. 2021a)) while dashed lines correspond to modeled radial profiles. Our final model includes an increase in C/O ratio beyond 20 au and a depletion of small dust and represents 1 Myr of chemistry. This model can simultaneously fit the flux, line ratios, and general morphology of the observed radial profiles of these complex organic molecules.

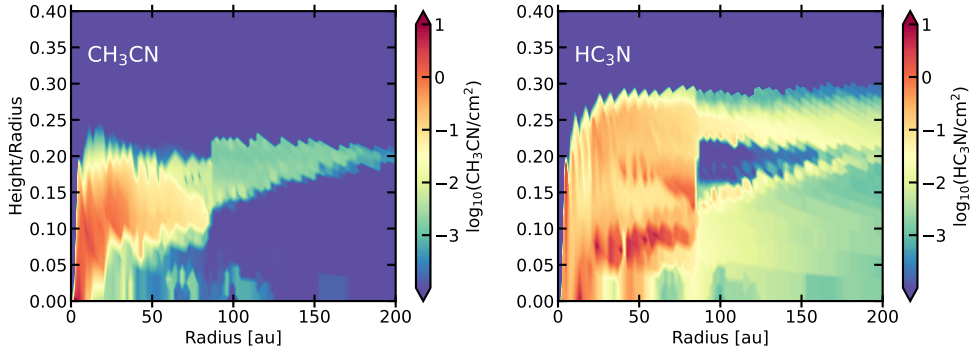

Figure 3. The radial and vertical number density distributions of CH_3CN and HC_3N The density distributions were determined by our final HD 163296 model with an increase in C/O ratio beyond 20 au and a depletion of small dust. This distribution produced the radial profiles shown in Figure 2. A z/r<0.1 is good approximation for the midplane of the disk, and both CH_3CN and HC_3N emit partially from the midplane. A comparison can be made with Figure 10 which lacks the inclusion of small dust depletion.

>1 can be explained by the natural evolution of dust and the observed high C-to-O ratios within protoplanetary disks. This environment could be extended to the inner disk in some cases, as studies such as Najita et al. 2011(Najita et al. 2011) and Anderson et al. 2021(Anderson et al. 2021) posit a higher than solar C-to-O ratio within the inner disk to account for Spitzer observations of HCN and C_2H_2 around T Tauri stars.

The implications of this end-stage chemistry are far-reaching. Primarily, we put forward a new chemically and physically coupled picture of planet formation and its direct impact on the chemistry of forming planet atmospheres. Within the early stages

of planet formation, pebble growth and accretion into solid planet cores has begun, and chemistry onto these cores are influenced primarily by the chemical make-up of large pebbles and their icy mantles. The chemistry active in the midplane during this stage of formation is dominated by X-rays and cosmic rays(Woitke et al. 2009). After timescales of order 1 Myr, at the end-stage of pebble formation, small grains have grown and settled towards the midplane, allowing for UV photons to penetrate deeper in the disk than previously assumed. This excess UV flux in concert with an above solar C-to-O ratio produces a carbon-rich gas phase cycle of production and destruction in the gas surrounding actively forming planets. Bright emission from CH_3CN, HC_3N and other carbon-rich molecules emitting at cold temperatures are a sign-post of this evolved chemical environment. These forming gas giants may accrete this surrounding gas and its chemical signature into their atmosphere, and may be responsible for high C-to-O measurements that have been observed in exo-planetary atmospheres as compared to their host star(Brewer et al. 2017). Secondly, the deeper penetration of UV photons pushes the CO and H_2 self-shielding layers deeper into the disk. Due to this, there are more ions such as C^+ and H^+ throughout the disk than would have been present with a regular (ISM) level of small dust surface area. As the ion-fraction increases so does the area of the disk that is subject to magneto-rotational instability (MRI). In our final model, the UV field increases by a factor of 3-5 in the atmosphere and between 1-2 near the midplane, and thirteen times more gas mass is MRI-active, most notably the gas midplane within 10 au, and then at a z/r=0.1-0.2 within 30 au (see Figure 4). This could be a source of accretion(Gammie and Ostriker 1996) for older disks. Our proposed UV-dominated carbon-rich gas phase chemistry is a major shift in our understanding of the astrochemistry of planet formation. This transition will have a strong effect on the composition of actively forming planets, disk MRI-activity, and subsequent disk accretion.

METHODS

OBSERVATIONS

For a thorough description of the observations and the techniques used to obtain the CLEAN-ed images and radial profiles of CH_3CN, HCN, and HC_3N towards HD 163296 see Czekala et al. 2021(Czekala et al. 2021), Law et al. 2021(Law et al. 2021a), and Öberg et al. 2021(Öberg et al. 2021). A description of the observations of CH_3CN towards TW Hya can be found in Loomis et al. 2018a(Loomis et al. 2018). A brief summary of these observations are as follows.

- HD 163296 -

The data for HD 163296 is from the MAPS large program (Project ID 2018.1.01055.L)(Öberg et al. 2021). The image cubes were produced using the `tclean` task in the Common Astronomy Software Applications (CASA) package, version 6.1.0(McMullin et al. 2007). Keplerian masks based on the disk geometric parameters

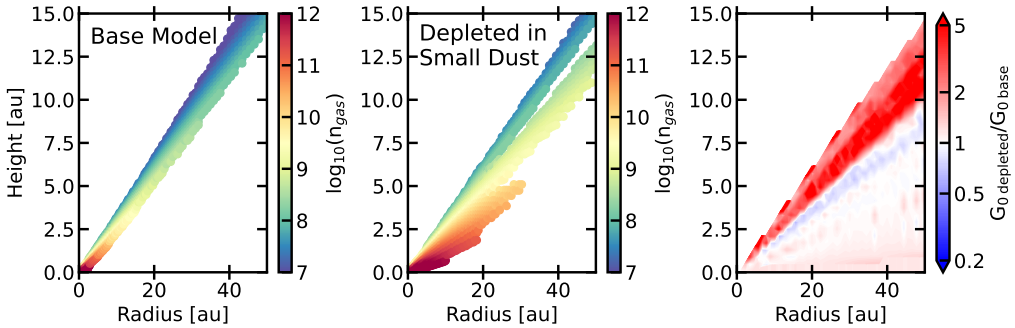

Figure 4. A comparison of the MRI active region within a non-elevated UV environment and an elevated UV environment. The two left-most plots show regions within the HD 163296 disk which are MRI activated in an environment where small dust is depleted by a factor of 10 in total mass (gas/dust = 5,000 middle plot) and where small dust is not depleted (gas/dust=500 left). The color corresponds to the gas density in mol/cm^3, highlighting the substantial increase in mass that is MRI-active. The right-most plot shows a comparison of the UV field strength through a 'regular' disk and a dust depleted disk. The UV field increases upwards of a factor of 3-5 in the atmosphere of the disk and 1-2 below a z/r=0.2. This has a notable effects on the chemistry of the midplane.

were used in the CLEANing process and the final images were then corrected for the Jorsater & van Moorsel effect to ensure that the image residuals are in units consistent with that of the CLEAN model. For all lines, we used the beam-circularized and uv-tapered images, which had synthesised beam sizes of 0."3. All radial intensity profiles were generated by deprojecting and azimuthally-averaging zeroth moment maps using the GoFish python package.

-TW HYA-

CH_3CN was observed towards TW Hya as a part of ALMA project 2016.1.01046.S. Each emission line was individually imaged using `CLEAN` and the synthesised beam for each transition were matched using small uv-tapers to 1.″05 x 0.″83. A Keplerian mask was used to extract the flux for each transition. See Loomis et al. 2018a(Loomis et al. 2018) for more details.

MODELING

Simple single point models of the disk environment were utilized to quickly and efficiently understand the chemical impacts of different physical and initial chemical conditions. Our chemical network is derived from Bosman et al. 2018(Bosman et al. 2018) which in turn is derived from the UMIST "RATE12" network(McElroy et al. 2013), and for this study we disregarded most grain-surface chemical reactions in order to isolate gas-phase formation of CH_3CN. After our results from the modeling suggested a higher gas/dust ratio and carbon content, we turned to more comprehensive thermo-chemical codes which model the thermal physics and chemical evolution throughout the whole disk. The code RAC2D (https://github.com/fjdu/rac-2d)(Du and Bergin 2014), was used to create models of the disks around TW Hya and HD 163296. The 2D temperature, density, and molecular abundance results were used to

simulate observations of each disk with a raytracing code: RADMC-3D(Dullemond et al. 2012). A brief description of the physical code of RAC2D is given below; a detailed description of the code can be found in Calahan et al 2021a(Calahan et al. 2021a).

RAC2D takes into account a gas and dust structure and stellar radiation field and computes the gas and dust temperature and chemical structure over time. Our model consists of three mass components: gas, small dust, and large dust grains. The spatial extent of each component is given by a global surface density distribution (Lynden-Bell and Pringle 1974), which is widely used in protoplanetary disk modeling and corresponds to the self-similar solution of a viscously evolved disk.

$$\Sigma(r) = \Sigma_c \left(\frac{r}{r_c}\right)^{-\gamma} \exp\left[-\left(\frac{r}{r_c}\right)^{2-\gamma}\right], \tag{1}$$

r_c is the characteristic radius at which the surface density is Σ_c/e where Σ_c is the characteristic surface density, and γ is the power-law index that describes the radial behavior of the surface density.

A 2D density profile for the gas and dust populations can be derived from the surface density profile and a scale height:

$$\rho(r,z) = \frac{\Sigma(r)}{\sqrt{2\pi}h(r)} \exp\left[-\frac{1}{2}\left(\frac{z}{h(r)}\right)^2\right], \tag{2}$$

$$h = h_c \left(\frac{r}{r_c}\right)^{\Psi}, \tag{3}$$

where h_c is the scale height at the characteristic radius, and Ψ is a power index that characterizes the flaring of the disk structure. The modeling parameters used for TW Hya and HD 163296 are shown in Table 1.

For both TW Hya and HD 163296 models, each dust population follows an Mathis, Rumpl, and Nordsieck (MRN) grain distribution $n(a) \propto a^{-3.5}$ (Mathis et al. 1977), where 'a' indicates the size of the grain. The small dust grains have radii between 5×10^{-3} - 1μm, and the large grains have radii between 5×10^{-3} - $10^3\mu$m. The large dust population is settled in the midplane with a smaller vertical extent and radial extent (gas extends ∼5 and 2.5 times above and beyond, respectively). This settled large grain population is the result of dust evolution, namely growth in concert with vertical settling to the midplane and radial drift. For the HD 163296 model, the large grain population has a unique, non-smooth, surface density profile that reproduces the millimeter continuum observations of the HD 163296 disk(Isella et al. 2018; Zhang et al. 2021). Opacity values for the dust are calculated based on Birnstiel et al. 2018(Birnstiel et al. 2018). Large dust grains consist of water ice(Warren and Brandt 2008), silicates(Draine 2003), troilites and refractory organics(Henning and Stognienko 1996). Small dust grains consist of 50% silicates and 50% refractory

organics. Further discussion on the modeling efforts for TW Hya can be found in Calahan et al. 2021a(Calahan et al. 2021a) and for HD 163296 in Calahan et al. 2021b(Calahan et al. 2021b).

The thermo-chemical model resulted in 2D distributions of the gas and dust temperature, density, and molecular abundances. These were used as inputs for the raytracing code RADMC-3D(Dullemond et al. 2012). The molecular properties of CH_3CN, HC_3N, and HCN were taken from the Leiden Atomic and Molecular Database (LAMDA(Schöier et al. 2005)), with some molecular parameters updated according to data from the Cologne Database for Molecular Spectroscopy (CDMS(Müller et al. 2001, 2005)). The result from RADMC-3D was a 3D image cube of the molecular emission across velocity space. We utilized `GoFish`(Teague 2019) to compress these 3D images into zeroth moment maps and radial profiles which were then directly compared to the azimuthally-averaged observations.

CHEMICAL REACTIONS

The chemical reaction network utilized in this work comes from Bosman et al. 2018(Bosman et al. 2018) which in turn relies on the Rate12 version of the UMIST Database for Astrochemistry(McElroy et al. 2013): a network that is widely used across astrochemical modeling efforts. In our network there are 6,302 gas phase reactions and we have limited the grain-surface reactions to twelve. We kept grain-surface reactions that involved the formation of H_2, CH_2OH, CH_3OH, CO_2, H_2O and NH_3 due to each of these species being well-studied in the laboratory and come with strong evidence for active two-body chemistry on dust grains(Allen and Robinson 1977; Hasegawa et al. 1992; Goumans et al. 2008; Ioppolo et al. 2008, 2010; Fuchs et al. 2009; Oba et al. 2012; Ruffle and Herbst 2001) (see Table 2). Both thermal adsorption and desorption are taken into account for every molecule in the network. Our network contains molecules with at most eleven carbon atoms, and at most twelve total atoms. We run our thermo-chemical model for 1 Myr as the CH_3CN and HC_3N chemistry reaches an equilibrium after this time period (see Supplementary Figure 3). In our evolved disk model, the main formation pathways for CH_3CN once the chemistry has reached equilibrium is as follows:

$$CH_3^+ + HCN \rightarrow CH_3CNH^+ + e^- \rightarrow CH_3CN + H$$

This reaction in the gas phase is the primary formation pathway for CH_3CN, thus there is a strong reliance on HCN existing in the gas phase even at cold temperatures below its measured sublimation temperature (∼85-103 K(Bergner et al. 2022)) and an ionization source (UV photons) to produce CH_3^+. HC_3N can be readily produced by a number of different ways including:

$$N + CH_2CCH \rightarrow HC_3N + H_2$$

$$CN + C_2H_2 \rightarrow HC_3N + H$$

Table 2. Dust Surface Reactions

Reaction	Reference
$gH + gH \rightarrow gH_2$	Hasegawa, Herbst, & Leung 1992(Hasegawa et al. 1992)
$gH + gOH \rightarrow gH_2O$	Ioppolo et al. 2010(Ioppolo et al. 2010)
$gH + gH_2O_2 \rightarrow gH_2O + gOH$	Ioppolo et al. 2008(Ioppolo et al. 2008)
$gH + gCH_3OH \rightarrow gH_2 + gCH_2OH$	Extrapolated from Fuchs et al. 2009(Fuchs et al. 2009)
$gH + gCH_2OH \rightarrow gCH_3OH$	Extrapolated from Fuchs et al. 2009(Fuchs et al. 2009)
$gH_2 + gOH \rightarrow gH_2O + gH$	Oba et al 2012(Oba et al. 2012)
$gOH + gCO \rightarrow gCO_2 + gH$ [a]	Ruffle & Herbst 2001(Ruffle and Herbst 2001)
$gO + gCO \rightarrow gCO_2$ [a]	Goumans & Brown 2008(Goumans et al. 2008)
$gO + gHCO \rightarrow gCO_2 + gH$	Goumans & Brown 2008(Goumans et al. 2008)
$gH + gNH_2 \rightarrow gNH_3$	Allen & Robinson 1977(Allen and Robinson 1977)

NOTE—The complete list dust surface reactions accounted for in this study. [a]Have additional special treatment for three body reactions

$$H + C_3N^- \rightarrow HC_3N + e^-$$

The formation of HC_3N strongly relies on the existence of carbon-rich molecules including radicals (CN) and ions (C_3N^-).

SUPPLEMENTARY INFORMATION

TW HYA

We additionally produced a thermo-chemical model representing the disk around T Tauri star TW Hya. TW Hya is approximately 10 Myrs old(Thi et al. 2010) and hosts the closest Class II disk at 59.9 pc(Gaia Collaboration et al. 2018). TW Hya has been widely observed in multiple gas and dust tracers with high spatial resolution ($\sim$10 au)(Andrews et al. 2012; Huang et al. 2018). It also exhibits bright CH_3CN coming from $\sim$33 K gas(Loomis et al. 2018). Our modeling efforts of TW Hya follow that of Calahan et al. 2021a(Calahan et al. 2021a) which sets up a thermo-chemical model of the disk by reproducing the spectral-energy distribution (SED), the full line intensity and morphology of seven CO isotopologue transitions, and an HD J=1-0 observation from the *Hershel* PACS instrument(Bergin et al. 2013). To reproduce all CO radial profiles as well as the HD flux, the small dust in the upper layers of the atmosphere of the TW Hya disk were effectively depleted slightly(Calahan et al. 2021a) due to having a slightly lower flaring angle than the gas population. This was enough small dust depletion to reproduce the available CH_3CN lines from Loomis et al. 2018a given a C/O ratio equal to 1.0 (see Figure 5). This disk is an additional piece of evidence supporting our evolved chemistry proposal.

IMPLICATIONS ON OTHER MOLECULES

This introduction of a late-stage photo-chemical equilibrium was motivated by observations of CH_3CN, HC_3N, and HCN. However, the late-stage chemistry would have an effect on other molecules as well. We predict in addition to these organic molecules, molecules such as C_XH, C_XH_2, and HC_XN will be abundant in the gas, enhanced by the cycle of carbon chemistry that reproduces observed CH_3CN and HC_3N. The main carbon carrier, CO, is largely unaffected by the increase in photo-chemistry. CO is largely in the gas phase in previous models that do not include this 'late-stage' chemistry and in the region in which CH_3CN was added into the gas, CO was already primarily in the gas phase. We find a slight depletion of CO in the upper atmosphere of the disk due to the CO photodissociation layer being pushed down, and there is a slight enhancement of CO in the midplane due to the UV-enhancement. However this accounts for less than 1% of the total abundance of CO thus did not have a strong impact on the modeled radial profiles. Another key molecule is H_2O. In our models, we do not initialize our model with H_2O, thus there is very little water to be affected by this 'late-stage' chemistry. Observational results of Du et al. 2017(Du et al. 2017) support this as they found a low overall abundance in H_2O in disks with a survey of 13 protoplanetary disks. CH_3CN nor HC_3N would be seen to be at a high abundance if gas-phase H_2O was in high abundance in the disk as it would disrupt the carbon-rich chemistry.

SED DEGENERACY

The depletion of small grains will affect the observed spectral energy distribution (SED) from each disk. TW Hya's dust population was not altered from that of Calahan et al. 2021a(Calahan et al. 2021a) and continues to match its observed SED. A depletion of a factor of 10 in the small dust population around HD 163296 would cause a dimming in the mid-infrared part of the SED. However, the small dust abundance, the distribution of dust grain size, and the assumed dust opacity sources are degenerate in the ways they may affect the disk SED. We modeled protoplanetary disk SEDs using the code TORUS(Harries et al. 2004, 2019). TORUS is a Monte Carlo radiative transfer code utilizing radiative equilibrium(Lucy 1999) and silicate grains(Draine and Lee 1984). In Figure 11, we show a series of SEDs produced from models motivated by our thermo-chemical model of HD 163296 including the stellar parameters and dust distribution in Table 1 from Calahan et al. 2021b(Calahan et al. 2021b). We find that by varying the minimum dust grain radius or the power law index, we can account for a factor of 10 in UV attenuation. The total population mass, grain size, and how the grain sizes are distributed are strongly degenerate and can result in uncertainties of the dust mass by a factor of at least 10. Thus our depletion of small dust continues to reproduce all previous observables including the SED.

MRI INSTABILITY

With the increase in UV flux deeper into the disk, more ions are created. Ions can be coupled with the magnetic fields that thread through the disk and interact with the bulk gas creating turbulence. This mechanism is called the magneto-rotational instability or MRI(Balbus and Hawley 1991). Magneto-hydrodynamical processes are assumed to be present throughout protoplanetary disks due to young star's active magnetic field, and are thought to be one of the main drivers of angular momentum transport (Chandrasekhar 1960). An MRI-active zone may drive the bulk of the mass transportation in the disk and activate accretion onto the star, two vital processes that determine the future of a young solar system. It is thought that planet formation may be aided within 'dead-zones' where MRI is non-active(Gressel et al. 2012). The magnetic Reynolds number (Re) and ambipolar diffusion term (Am) are two quantities that help quantify the presence of an MRI-active zone. The Reynolds number quantifies the level of coupling between ionized gas and magnetic fields and is defined as

$$Re \equiv \frac{c_s h}{D} \approx 1 \left(\frac{\chi_e}{10^{-13}}\right) \left(\frac{T}{100\ \mathrm{K}}\right)^{1/2} \left(\frac{a}{\mathrm{AU}}\right)^{3/2}, \tag{4}$$

where c_s is the sound speed, h is the scale height of the disk, D is the magnetic diffusivity parameter, χ_e is the electron abundance, T temperature and a radial location in the disk (Perez-Becker and Chiang 2011). The ambipolar diffusion term describes the coupling of ionized molecules and their interaction with neutral gas particles:

$$Am \equiv \frac{\chi_i n_{\mathrm{H_2}} \beta_{\mathrm{in}}}{\Omega} \approx 1 \left(\frac{\chi_i}{10^{-8}}\right) \left(\frac{n_{\mathrm{H_2}}}{10^{10}\mathrm{cm}^{-3}}\right) \left(\frac{a}{\mathrm{AU}}\right)^{3/2}, \tag{5}$$

where χ_i is the ion abundance, $n_{\mathrm{H_2}}$ is the number density of H_2 atoms, Ω is the dynamical time, β_{in} is the collisional rate coefficient for singly charged species to share momentum with neutral species, and a is the radial location in the disk (Draine et al. 1983; Perez-Becker and Chiang 2011). For MRI to act as a turbulent driver of neutral gas, both Re and Am must be sufficiently high. Simulations show that values between 0.1-100 for Am can trigger significant coupling between ions and neutrals (Hawley and Stone 1998; Bai and Stone 2011). Models by Flock et al. 2012(Flock et al. 2012) suggest $Re \approx$ 3,300-5,000 is required to sustain sufficient turbulence with a critical Re = 3,000. In our work, we assume a combined Am >100 and Re > 3,000 to signify an MRI-active zone.

We calculate the regions in which the MRI is active in the HD 163296 disk in our models with an early-stage physical environment and a late-stage environment (signified by a depletion in the small dust population mass) in Figure 8. Our solution allows for an increase of UV flux in the atmosphere by a factor of 3-5. More of the disk becomes ion-rich due to the CO and H_2 self-shielding layers being located deeper into the disk. The increase in the ion and electron abundance (χ_i, χ_e) are the key factors that enhance the Re and Am values and thus produce additional MRI activity (see Figure 8). As a result, thirteen times more mass within the disk

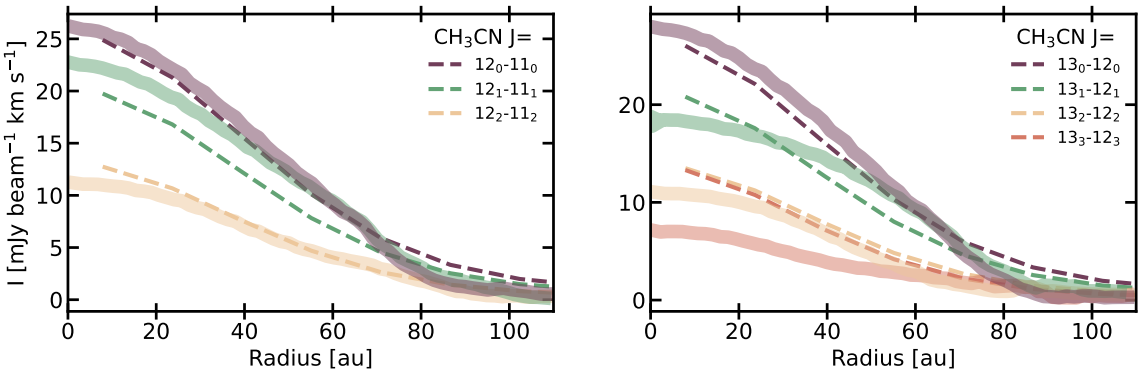

Figure 5. A comparison of observed CH_3CN(Loomis et al. 2018) towards TW Hya and a thermo-chemical model. The model is run for 1 Myr with a gas-to-dust ratio equal to 250 and a C-to-O ratio equal to 1.0. Observed emission is shown as the solid lines while modeled results are the dashed lines. The left and right panels show different J_K transitions.

becomes MRI-active including within the midplane. In the base model representing early stages of disk chemistry, the MRI activity at the midplane extends to 4 au. By depleting the small dust population by an order of magnitude, the MRI activity at the midplane then extends out to ∼10 au. This increase in MRI activity can contribute to the reason behind why older disk systems, such as TW Hya, are actively accreting. Meridional flows have been identified in the HD 163296 disk located at two of the largest dust gaps (approx. 45 and 86 AU)(Teague et al. 2019) and these vertical flows are coincident with the lower vertical limit of the MRI-active zone. The MRI activation could have an effect on the height or continue to drive meridional flows. Turbulence measurements of the HD 163296 disk have been derived in Flaherty et al. 2015 and 2017(Flaherty et al. 2015, 2017) using molecular tracers, and they find turbulent velocities to be 5% or less of the sound speed between 30-300 au and at all measured heights. It is not yet clear whether our MRI prediction is in tension with the observational evidence of low turbulence in HD 163296, more work needs to be done on the modeling of how MRI-active regions drive turbulence and more observational constraints are needed to constrain the inner 40 au where we find the strongest MRI-activity.

SUPPLEMENTARY FIGURES

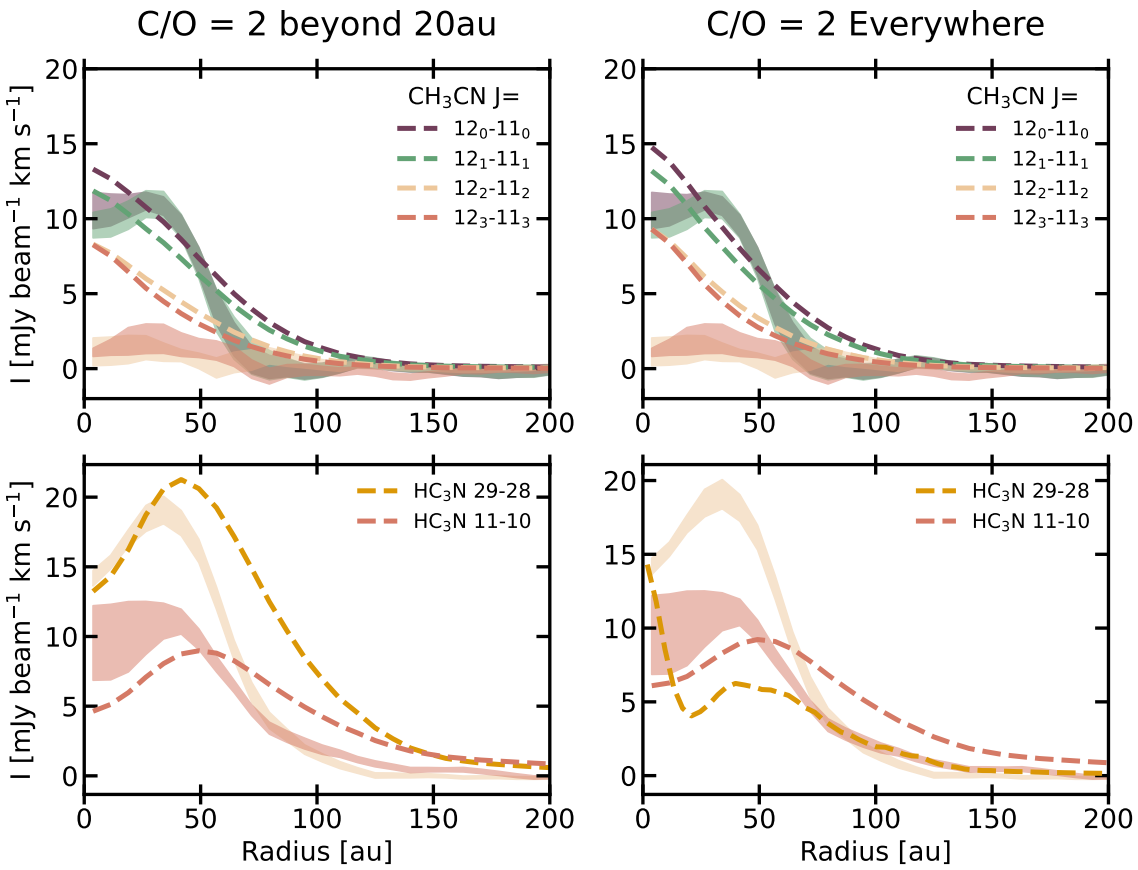

Figure 6. A comparison of two HD 163296 disk models with varying C-to-O ratios. The final model has a C-to-O = 0.47 within 20 au and C-to-O = 2 beyond 20 au (left). The comparison model has a C-to-O ratio equal 2 throughout the entire disk. Dashed lines are modeled radial intensity profiles while the thick line in the background are observations, with the thickness corresponding to the uncertainty of the flux. In our final model, the C-to-O ratio is equal to what is found in the ISM, 0.47.

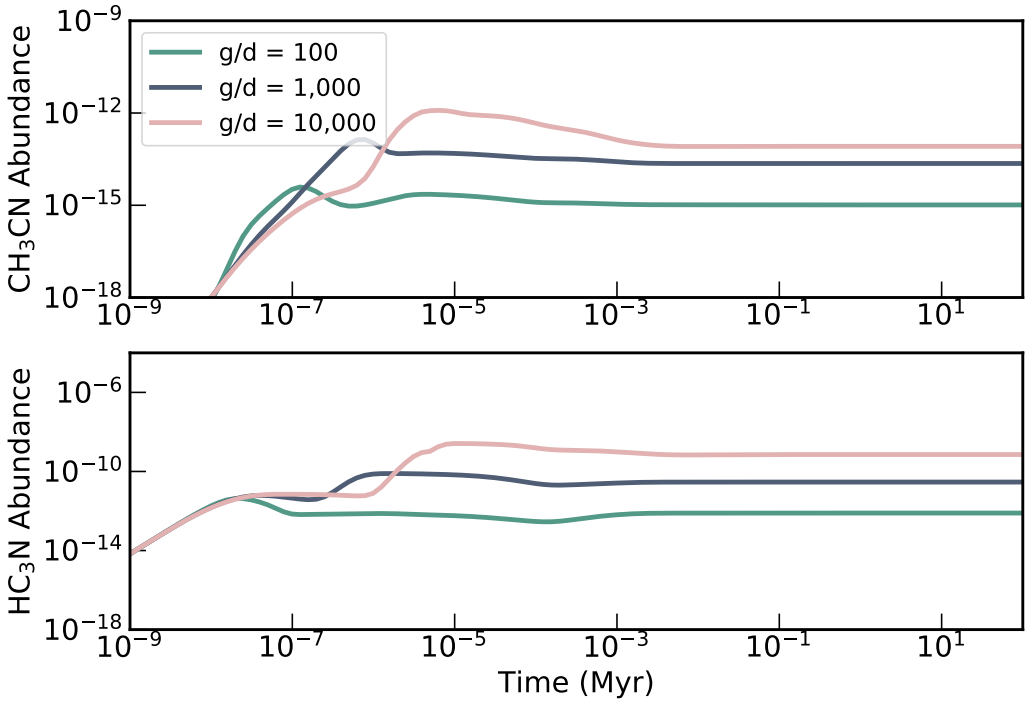

Figure 7. The evolution of CH_3CN and HC_3N abundances relative to H_2 given different gas to dust ratios. This considers an environment with a 35 K gas and $\mathbf{5 \times 10^{11}}$ mol/cm^3 gas density following our chemical network. The top panel shows the temporal evolution of CH_3CN abundance while the bottom shows the evolution of HC_3N

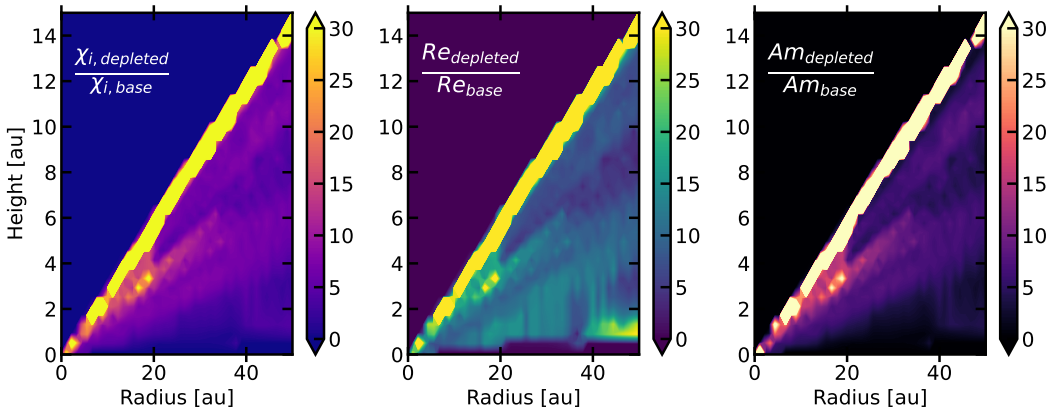

Figure 8. A comparison of the terms that effect the MRI strength in two distict models. The final ion abundance (χ_i left) calculated Reynolds number (Re, middle) and ambipolar diffusion term (Am, right) are shown in a model depleted of small dust (gas-to-dust = 5,000) versus a baseline model (gas-to-dust = 500). The depleted model corresponds to the model that reproduces observations of CH_3CN, HCN, and HC_3N, see Figure 2 of main text.

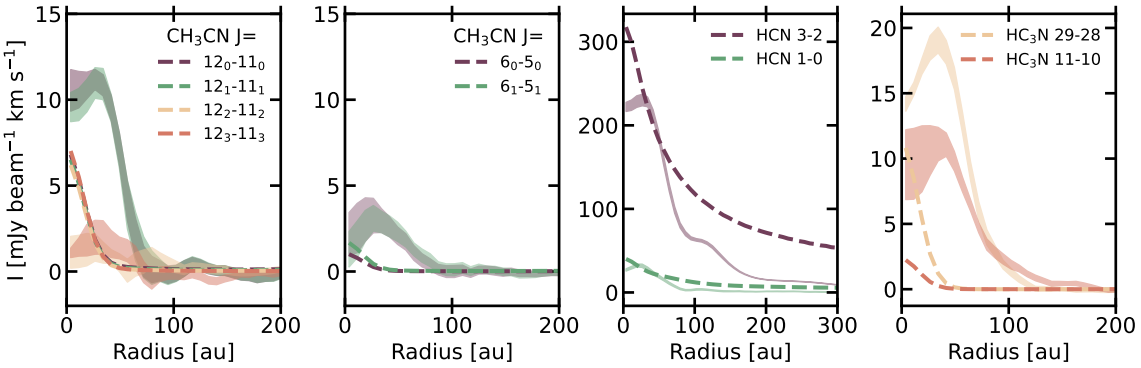

Figure 9. An HD 163296 model with an elevated C-to-O ratio and normal gas-to-dust ratio in the atmosphere. The model is represented by dashed lines while observations are the thick low opacity lines, where the thickness corresponds to the uncertainty in the flux. The model predicts that each K-line for CH_3CN J=12-11 have nearly identical morphology and intensities. HC_3N is predicted to have a centrally peaked radial intensity profile while observations show a plateau or central dip. By simply decreasing the total mass thus total surface density of the small dust by a factor of 10, the model is much more consistent with observations across all three molecules and their multiple transitions.

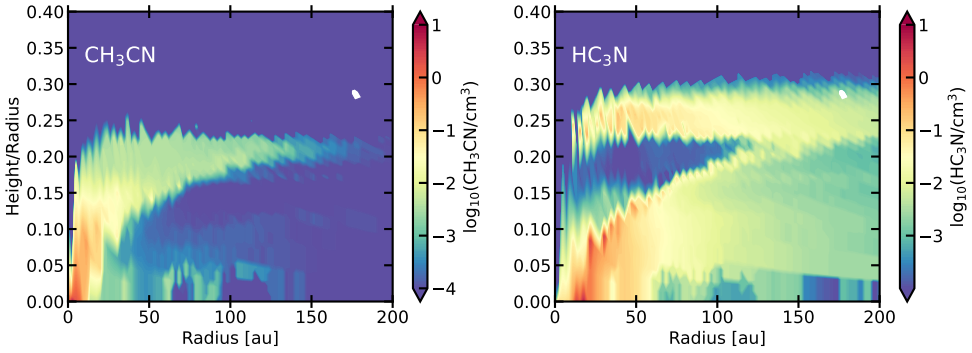

Figure 10. The radial and vertical number density distributions of CH_3CN and HC_3N in a model with a high C-to-O ratio and normal gas-to-dust ratio. C-to-O is equal to 2 throughout the whole disk, and the atmospheric gas-to-dust ratio is equal to 500 (corresponding to the model results in Figure 9). This is contrasted with Figure 3, where there is more organic emission deeper in the disk.

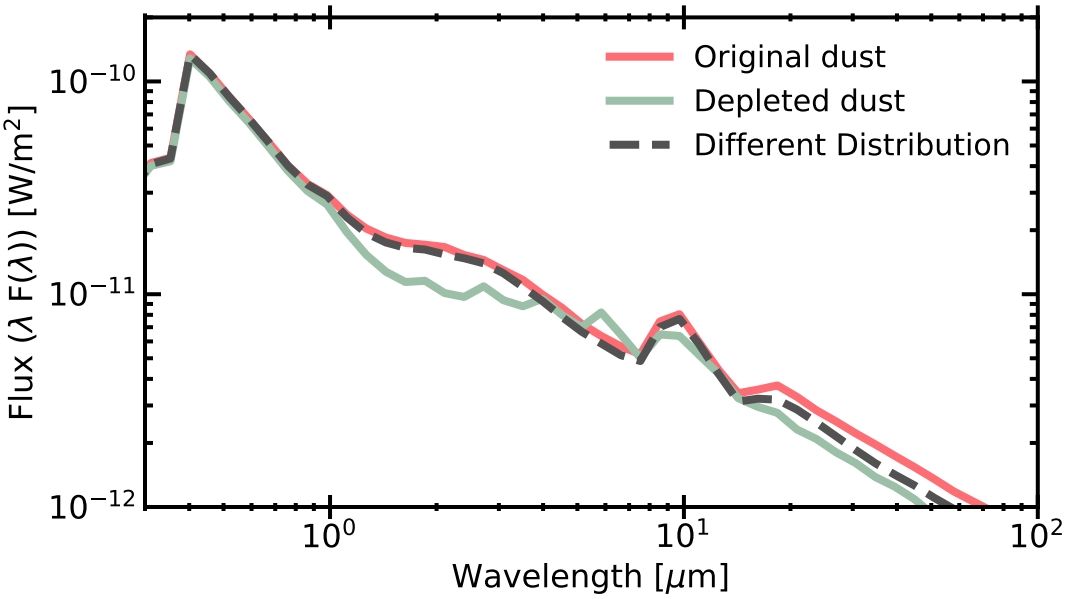

Figure 11. Three simulated SEDs for different protoplanetary disk dust populations. The 'depleted dust' model has 10 times less mass in the small dust population than the 'Original dust' model. By altering the UV attenuation via increasing the minimum dust radius from 0.005 μm to 0.1 μm (dashed grey line) we reproduce the SED features and intensity as seen in the 'original' model.

1. ACKNOWLEDGEMENTS

Jenny Calahan is the corresponding author and can be contacted via jcalahan@umich.edu

J.K.C. acknowledges support from the National Science Foundation Graduate Research Fellowship under Grant No. DGE 1256260 and the National Aeronautics and Space Administration FINESST grant, under Grant no. 80NSSC19K1534. E.A.B. acknowledges support from NSF AAG Grant #1907653. A.D.B. acknowledges support from NSF AAG Grant #1907653. E.A.R. acknowledges support from NSF AST 1830728. Support for J. H. was provided by NASA through the NASA Hubble Fellowship grant #HST-HF2-51460.001-A awarded by the Space Telescope Science Institute, which is operated by the Association of Universities for Research in Astronomy, Inc., for NASA, under contract NAS5-26555. This work was supported by a grant from the Simons Foundation 686302 and by an award from the Simons Foundation 321183FY19, KÖ. This material is based upon work supported by the National Science Foundation under Grant No. AST-1907832. J.D.I. acknowledges support from an STFC Ernest Rutherford Fellowship (ST/W004119/1) and a University Academic Fellowship from the University of Leeds. C.W. acknowledges financial support from the University of Leeds, the Science and Technology Facilities Council, and UK Research and Innovation (grant numbers ST/T000287/1 and MR/T040726/1). V.V.G. gratefully acknowledges support from FONDECYT Regular 1221352, ANID BASAL projects ACE210002 and FB210003, and ANID, – Millennium Science Initiative Program – NCN19_171.

We thank Tim Harries for help with and providing access to the TORUS modeling program.

DATA AVAILABILITY

The data that support the findings of this study can be obtained as part of the MAPS program and are publicly available via alma-maps.info. Data regarding TW Hya can be obtained via data-rich figures in Calahan et al 2021 published on the online publication of the Astrophysical Journal article.

This paper makes use of the following ALMA data: ADS/JAO.ALMA#2018.1.01055.L. and 2016.1.01046.S ALMA is a partnership of ESO (representing its member states), NSF (USA) and NINS (Japan), together with NRC (Canada), MOST and ASIAA (Taiwan), and KASI (Republic of Korea), in cooperation with the Republic of Chile. The Joint ALMA Observatory is operated by ESO, AUI/NRAO and NAOJ. The National Radio Astronomy Observatory is a facility of the National Science Foundation operated under cooperative agreement by Associated Universities, Inc.

CODE AVAILABILITY

This study relied on the following publicly available coding packages: rac2d: https://github.com/fjdu/rac-2d, RADMC-3D: https://www.ita.uni-heidelberg.de/ dullemond/software/radmc-3d/, and GoFish: https://github.com/richteague/gofish. TORUS is a private code developed by Tim Harries and collaborators.

REFERENCES

M. Allen and G. W. Robinson. The molecular composition of dense interstellar clouds. *ApJ*, 212:396–415, March 1977. https://doi.org/10.1086/155059.

Dana E. Anderson, Geoffrey A. Blake, L. Ilsedore Cleeves, Edwin A. Bergin, Ke Zhang, Kamber R. Schwarz, Colette Salyk, and Arthur D. Bosman. Observing Carbon and Oxygen Carriers in Protoplanetary Disks at Mid-infrared Wavelengths. *ApJ*, 909(1):55, March 2021. https://doi.org/10.3847/1538-4357/abd9c1.

Sean M. Andrews and Tilman Birnstiel. Dust Evolution in Protoplanetary Disks. In Hans J. Deeg and Juan Antonio Belmonte, editors, *Handbook of Exoplanets*, page 136. 2018. https://doi.org/10.1007/978-3-319-55333-7_136.

Sean M. Andrews, David J. Wilner, A. M. Hughes, Chunhua Qi, Katherine A. Rosenfeld, Karin I. Öberg, T. Birnstiel, Catherine Espaillat, Lucas A. Cieza, Jonathan P. Williams, Shin-Yi Lin, and Paul T. P. Ho. The TW Hya Disk at 870 μm: Comparison of CO and Dust Radial Structures. *ApJ*, 744(2):162, January 2012. https://doi.org/10.1088/0004-637X/744/2/162.

Sean M. Andrews, Jane Huang, Laura M. Pérez, Andrea Isella, Cornelis P. Dullemond, Nicolás T. Kurtovic, Viviana V. Guzmán, John M. Carpenter, David J. Wilner, Shangjia Zhang, Zhaohuan Zhu, Tilman Birnstiel, Xue-Ning Bai, Myriam Benisty, A. Meredith Hughes, Karin I. Öberg, and Luca Ricci. The Disk Substructures at High Angular Resolution Project (DSHARP). I. Motivation, Sample, Calibration, and Overview. *ApJL*, 869(2):L41, December 2018. https://doi.org/10.3847/2041-8213/aaf741.

M. Ansdell, J. P. Williams, L. Trapman, S. E. van Terwisga, S. Facchini, C. F. Manara, N. van der Marel, A. Miotello, M. Tazzari, M. Hogerheijde, G. Guidi, L. Testi, and E. F. van Dishoeck. ALMA Survey of Lupus Protoplanetary Disks. II. Gas Disk Radii. *ApJ*, 859(1): 21, May 2018. https://doi.org/10.3847/1538-4357/aab890.

M. Asplund, A. M. Amarsi, and N. Grevesse. The chemical make-up of the Sun: A 2020 vision. *A&A*, 653: A141, September 2021. https://doi.org/10.1051/0004-6361/202140445.

Xue-Ning Bai and James M. Stone. Effect of Ambipolar Diffusion on the Nonlinear Evolution of Magnetorotational Instability in Weakly Ionized Disks. *ApJ*, 736(2):144, August 2011. https://doi.org/10.1088/0004-637X/736/2/144.

Steven A. Balbus and John F. Hawley. A Powerful Local Shear Instability in Weakly Magnetized Disks. I. Linear Analysis. *ApJ*, 376:214, July 1991. https://doi.org/10.1086/170270.

Romain Basalgète, Antonio Jesus Ocaña, Géraldine Féraud, Claire Romanzin, Laurent Philippe, Xavier Michaut, Jean-Hugues Fillion, and Mathieu Bertin. Photodesorption of Acetonitrile CH_3CN in UV-irradiated Regions of the Interstellar Medium: Experimental Evidence. *ApJ*, 922(2):213, December 2021. https://doi.org/10.3847/1538-4357/ac2d93.

Edwin A. Bergin, L. Ilsedore Cleeves, Uma Gorti, Ke Zhang, Geoffrey A. Blake, Joel D. Green, Sean M. Andrews, II Evans, Neal J., Thomas Henning, and Karin Öberg. An old disk still capable of forming a planetary system. *Nature*, 493(7434):644–646, Jan 2013. https://doi.org/10.1038/nature11805.

Jennifer B. Bergner and Fred Ciesla. Ice Inheritance in Dynamical Disk Models. *ApJ*, 919(1):45, September 2021. https://doi.org/10.3847/1538-4357/ac0fd7.

Jennifer B. Bergner, Viviana G. Guzmán, Karin I. Öberg, Ryan A. Loomis, and Jamila Pegues. A Survey of CH_3CN and HC_3N in Protoplanetary Disks. *ApJ*, 857(1):69, April 2018. https://doi.org/10.3847/1538-4357/aab664.

Jennifer B. Bergner, Karin I. Öberg, Edwin A. Bergin, Ryan A. Loomis, Jamila Pegues, and Chunhua Qi. A Survey of C_2H, HCN, and $C^{18}O$ in Protoplanetary Disks. *ApJ*, 876(1):25, May 2019. https://doi.org/10.3847/1538-4357/ab141e.

Jennifer B. Bergner, Karin I. Öberg, Viviana V. Guzmán, Charles J. Law, Ryan A. Loomis, Gianni Cataldi, Arthur D. Bosman, Yuri Aikawa, Sean M. Andrews, Edwin A. Bergin, Alice S. Booth, L. Ilsedore Cleeves, Ian Czekala, Jane Huang, John D. Ilee, Romane Le Gal, Feng Long, Hideko Nomura, François Ménard, Chunhua Qi, Kamber R. Schwarz, Richard Teague, Takashi Tsukagoshi, Catherine Walsh, David J. Wilner, and Yoshihide Yamato. Molecules with ALMA at Planet-forming Scales (MAPS). XI. CN and HCN as Tracers of Photochemistry in Disks. *ApJS*, 257(1):11, November 2021. https://doi.org/10.3847/1538-4365/ac143a.

Jennifer B. Bergner, Mahesh Rajappan, and Karin I. Öberg. HCN Snow Lines in Protoplanetary Disks: Constraints from Ice Desorption Experiments. *ApJ*, 933(2):206, July 2022. https://doi.org/10.3847/1538-4357/ac771e.

T. Birnstiel, S. M. Andrews, and B. Ercolano. Can grain growth explain transition disks? *A&A*, 544:A79, August 2012. https://doi.org/10.1051/0004-6361/201219262.

Tilman Birnstiel, Cornelis P. Dullemond, Zhaohuan Zhu, Sean M. Andrews, Xue-Ning Bai, David J. Wilner, John M. Carpenter, Jane Huang, Andrea Isella, Myriam Benisty, Laura M. Pérez, and Shangjia Zhang. The Disk Substructures at High Angular Resolution Project (DSHARP). V. Interpreting ALMA Maps of Protoplanetary Disks in Terms of a Dust Model. *ApJL*, 869(2):L45, December 2018. https://doi.org/10.3847/2041-8213/aaf743.

Alice S. Booth, Benoît Tabone, John D. Ilee, Catherine Walsh, Yuri Aikawa, Sean M. Andrews, Jaehan Bae, Edwin A. Bergin, Jennifer B. Bergner, Arthur D. Bosman, Jenny K. Calahan, Gianni Cataldi, L. Ilsedore Cleeves, Ian Czekala, Viviana V. Guzmán, Jane Huang, Charles J. Law, Romane Le Gal, Feng Long, Ryan A. Loomis, François Ménard, Hideko Nomura, Karin I. Öberg, Chunhua Qi, Kamber R. Schwarz, Richard Teague, Takashi Tsukagoshi, David J. Wilner, Yoshihide Yamato, and Ke Zhang. Molecules with ALMA at Planet-forming Scales (MAPS). XVI. Characterizing the Impact of the Molecular Wind on the Evolution of the HD 163296 System. *ApJS*, 257(1):16, November 2021. https://doi.org/10.3847/1538-4365/ac1ad4.

Arthur D. Bosman, Catherine Walsh, and Ewine F. van Dishoeck. CO destruction in protoplanetary disk midplanes: Inside versus outside the CO snow surface. *A&A*, 618:A182, October 2018. https://doi.org/10.1051/0004-6361/201833497.

Arthur D. Bosman, Felipe Alarcón, Edwin A. Bergin, Ke Zhang, Merel L. R. van't Hoff, Karin I. Öberg, Viviana V. Guzmán, Catherine Walsh, Yuri Aikawa, Sean M. Andrews, Jennifer B. Bergner, Alice S. Booth, Gianni Cataldi, L. Ilsedore Cleeves, Ian Czekala, Kenji Furuya, Jane Huang, John D. Ilee, Charles J. Law, Romane Le Gal, Yao Liu, Feng Long, Ryan A. Loomis, François Ménard, Hideko Nomura, Chunhua Qi, Kamber R. Schwarz, Richard Teague, Takashi Tsukagoshi, Yoshihide Yamato, and David J. Wilner. Molecules with ALMA at Planet-forming Scales (MAPS). VII. Substellar O/H and C/H and Superstellar C/O in Planet-feeding Gas. *ApJS*, 257(1):7, November 2021a. https://doi.org/10.3847/1538-4365/ac1435.

Arthur D. Bosman, Felipe Alarcón, Ke Zhang, and Edwin A. Bergin. Destruction of Refractory Carbon Grains Drives the Final Stage of Protoplanetary Disk Chemistry. *ApJ*, 910(1):3, March 2021b. https://doi.org/10.3847/1538-4357/abe127.

John M. Brewer, Debra A. Fischer, and Nikku Madhusudhan. C/O and O/H Ratios Suggest Some Hot Jupiters Originate Beyond the Snow Line. *AJ*, 153(2):83, February 2017. https://doi.org/10.3847/1538-3881/153/2/83.

Jenny K. Calahan, Edwin Bergin, Ke Zhang, Richard Teague, Ilsedore Cleeves, Jennifer Bergner, Geoffrey A. Blake, Paolo Cazzoletti, Viviana Guzmán, Michiel R. Hogerheijde, Jane Huang, Mihkel Kama, Ryan Loomis, Karin Öberg, Charlie Qi, Ewine F. van Dishoeck, Jeroen Terwisscha van Scheltinga, Catherine Walsh, and David Wilner. The TW Hya Rosetta Stone Project. III. Resolving the Gaseous Thermal Profile of the Disk. *ApJ*, 908 (1):8, February 2021a. https://doi.org/10.3847/1538-4357/abd255.

Jenny K. Calahan, Edwin A. Bergin, Ke Zhang, Kamber R. Schwarz, Karin I. Öberg, Viviana V. Guzmán, Catherine Walsh, Yuri Aikawa, Felipe Alarcón, Sean M. Andrews, Jaehan Bae, Jennifer B. Bergner, Alice S. Booth, Arthur D. Bosman, Gianni Cataldi, Ian Czekala, Jane Huang, John D. Ilee, Charles J. Law, Romane Le Gal, Feng Long, Ryan A. Loomis, François Ménard, Hideko Nomura, Chunhua Qi, Richard Teague, Merel L. R. van't Hoff, David J. Wilner, and Yoshihide Yamato. Molecules with ALMA at Planet-forming Scales (MAPS). XVII. Determining the 2D Thermal Structure of the HD 163296 Disk. *ApJS*, 257(1):17, November 2021b. https://doi.org/10.3847/1538-4365/ac143f.

Alessandra Canta, Richard Teague, Romane Le Gal, and Karin I. Öberg. The First Detection of CH_2CN in a Protoplanetary Disk. *ApJ*, 922(1):62, November 2021. https://doi.org/10.3847/1538-4357/ac23da.

S. Chandrasekhar. The Stability of Non-Dissipative Couette Flow in Hydromagnetics. *Proceedings of the National Academy of Science*, 46(2): 253–257, February 1960. https://doi.org/10.1073/pnas.46.2.253.

Edwige Chapillon, Anne Dutrey, Stéphane Guilloteau, Vincent Piétu, Valentine Wakelam, Franck Hersant, Fréderic Gueth, Thomas Henning, Ralf Launhardt, Katharina Schreyer, and Dmitry Semenov. Chemistry in Disks. VII. First Detection of HC_3N in Protoplanetary Disks. *ApJ*, 756(1):58, September 2012. https://doi.org/10.1088/0004-637X/756/1/58.

L. Ilsedore Cleeves, Ryan A. Loomis, Richard Teague, Edwin A. Bergin, David J. Wilner, Jennifer B. Bergner, Geoffrey A. Blake, Jenny K. Calahan, Paolo Cazzoletti, Ewine F. van Dishoeck, Viviana V. Guzmán, Michiel R. Hogerheijde, Jane Huang, Mihkel Kama, Karin I. Öberg, Chunhua Qi, Jeroen Terwisscha van Scheltinga, and Catherine Walsh. The TW Hya Rosetta Stone Project IV: A Hydrocarbon-rich Disk Atmosphere. *ApJ*, 911(1):29, April 2021. https://doi.org/10.3847/1538-4357/abe862.

Maria Angela Corazzi, John Robert Brucato, Giovanni Poggiali, Linda Podio, Davide Fedele, and Claudio Codella. Thermal Desorption of Astrophysically Relevant Ice Mixtures of Acetaldehyde and Acetonitrile from Olivine Dust. *ApJ*, 913(2):128, June 2021. https://doi.org/10.3847/1538-4357/abf6d3.

Ian Czekala, Ryan A. Loomis, Richard Teague, Alice S. Booth, Jane Huang, Gianni Cataldi, John D. Ilee, Charles J. Law, Catherine Walsh, Arthur D. Bosman, Viviana V. Guzmán, Romane Le Gal, Karin I. Öberg, Yoshihide Yamato, Yuri Aikawa, Sean M. Andrews, Jaehan Bae, Edwin A. Bergin, Jennifer B. Bergner, L. Ilsedore Cleeves, Nicolas T. Kurtovic, François Ménard, Hideko Nomura, Laura M. Pérez, Chunhua Qi, Kamber R. Schwarz, Takashi Tsukagoshi, Abygail R. Waggoner, David J. Wilner, and Ke Zhang. Molecules with ALMA at Planet-forming Scales (MAPS). II. CLEAN Strategies for Synthesizing Images of Molecular Line Emission in Protoplanetary Disks. *ApJS*, 257(1):2, November 2021. https://doi.org/10.3847/1538-4365/ac1430.

B. T. Draine. Interstellar Dust Grains. *ARA&A*, 41:241–289, January 2003. https://doi.org/10.1146/annurev.astro.41.011802.094840.

B. T. Draine and H. M. Lee. Optical Properties of Interstellar Graphite and Silicate Grains. *ApJ*, 285:89, October 1984. https://doi.org/10.1086/162480.

B. T. Draine, W. G. Roberge, and A. Dalgarno. Magnetohydrodynamic shock waves in molecular clouds. *ApJ*, 264:485–507, January 1983. https://doi.org/10.1086/160617.

Fujun Du and Edwin A. Bergin. Water Vapor Distribution in Protoplanetary Disks. *ApJ*, 792(1):2, Sep 2014. https://doi.org/10.1088/0004-637X/792/1/2.

Fujun Du, Edwin Anthony Bergin, Michiel Hogerheijde, Ewine F. van Dishoeck, Geoff Blake, Simon Bruderer, Ilse Cleeves, Carsten Dominik, Davide Fedele, Dariusz C. Lis, Gary Melnick, David Neufeld, John Pearson, and Umut Yıldız. Survey of Cold Water Lines in Protoplanetary Disks: Indications of Systematic Volatile Depletion. *ApJ*, 842(2):98, June 2017. https://doi.org/10.3847/1538-4357/aa70ee.

C. P. Dullemond, A. Juhasz, A. Pohl, F. Sereshti, R. Shetty, T. Peters, B. Commercon, and M. Flock. RADMC-3D: A multi-purpose radiative transfer tool. Astrophysics Source Code Library, February 2012.

Kevin M. Flaherty, A. Meredith Hughes, Katherine A. Rosenfeld, Sean M. Andrews, Eugene Chiang, Jacob B. Simon, Skylar Kerzner, and David J. Wilner. Weak Turbulence in the HD 163296 Protoplanetary Disk Revealed by ALMA CO Observations. *ApJ*, 813 (2):99, November 2015. https://doi.org/10.1088/0004-637X/813/2/99.

Kevin M. Flaherty, A. Meredith Hughes, Sanaea C. Rose, Jacob B. Simon, Chunhua Qi, Sean M. Andrews, Ágnes Kóspál, David J. Wilner, Eugene Chiang, Philip J. Armitage, and Xue-ning Bai. A Three-dimensional View of Turbulence: Constraints on Turbulent Motions in the HD 163296 Protoplanetary Disk Using DCO^+. *ApJ*, 843(2):150, July 2017. https://doi.org/10.3847/1538-4357/aa79f9.

M. Flock, Th. Henning, and H. Klahr. Turbulence in Weakly Ionized Protoplanetary Disks. *ApJ*, 761(2):95, December 2012. https://doi.org/10.1088/0004-637X/761/2/95.

G. W. Fuchs, H. M. Cuppen, S. Ioppolo, C. Romanzin, S. E. Bisschop, S. Andersson, E. F. van Dishoeck, and H. Linnartz. Hydrogenation reactions in interstellar CO ice analogues. A combined experimental/theoretical approach. *A&A*, 505(2):629–639, October 2009. https://doi.org/10.1051/0004-6361/200810784.

Gaia Collaboration, A. G. A. Brown, A. Vallenari, T. Prusti, J. H. J. de Bruijne, C. Babusiaux, C. A. L. Bailer-Jones, M. Biermann, D. W. Evans, L. Eyer, F. Jansen, C. Jordi, S. A. Klioner, U. Lammers, L. Lindegren, X. Luri, F. Mignard, C. Panem, D. Pourbaix, S. Randich, P. Sartoretti, H. I. Siddiqui, C. Soubiran, F. van Leeuwen, N. A. Walton, F. Arenou, U. Bastian, M. Cropper, R. Drimmel, D. Katz, M. G. Lattanzi, J. Bakker, C. Cacciari, J. Castañeda, L. Chaoul, N. Cheek, F. De Angeli, C. Fabricius, R. Guerra, B. Holl, E. Masana, R. Messineo, N. Mowlavi, K. Nienartowicz, P. Panuzzo, J. Portell, M. Riello, G. M. Seabroke, P. Tanga, F. Thévenin, G. Gracia-Abril, G. Comoretto, M. Garcia-Reinaldos, D. Teyssier, M. Altmann, R. Andrae, M. Audard, I. Bellas-Velidis, K. Benson, J. Berthier, R. Blomme, P. Burgess, G. Busso, B. Carry, A. Cellino, G. Clementini, M. Clotet, O. Creevey, M. Davidson, J. De Ridder, L. Delchambre, A. Dell'Oro, C. Ducourant, J. Fernández-Hernández, M. Fouesneau, Y. Frémat, L. Galluccio, M. García-Torres, J. González-Núñez, J. J. González-Vidal, E. Gosset, L. P. Guy, J. L. Halbwachs, N. C. Hambly, D. L. Harrison, J. Hernández, D. Hestroffer, S. T. Hodgkin, A. Hutton, G. Jasniewicz, A. Jean-Antoine-Piccolo, S. Jordan, A. J. Korn, A. Krone-Martins, A. C. Lanzafame, T. Lebzelter, W. Löffler, M. Manteiga, P. M. Marrese, J. M. Martín-Fleitas, A. Moitinho, A. Mora, K. Muinonen, J. Osinde, E. Pancino, T. Pauwels, J. M. Petit, A. Recio-Blanco, P. J. Richards, L. Rimoldini, A. C. Robin, L. M. Sarro, C. Siopis, M. Smith, A. Sozzetti, M. Süveges, J. Torra, W. van Reeven, U. Abbas, A. Abreu Aramburu, S. Accart, C. Aerts, G. Altavilla, M. A. Álvarez, R. Alvarez, J. Alves, R. I. Anderson, A. H. Andrei, E. Anglada Varela, E. Antiche, T. Antoja, B. Arcay, T. L. Astraatmadja, N. Bach, S. G. Baker, L. Balaguer-Núñez, P. Balm, C. Barache, C. Barata,

Charles F. Gammie and Eve C. Ostriker. Can Nonlinear Hydromagnetic Waves Support a Self-gravitating Cloud? *ApJ*, 466:814, August 1996. https://doi.org/10.1086/177556.

Paul F. Goldsmith and William D. Langer. Population Diagram Analysis of Molecular Line Emission. *ApJ*, 517 (1):209–225, May 1999. https://doi.org/10.1086/307195.

T. P. M. Goumans, Madeeha A. Uppal, and Wendy A. Brown. Formation of CO_2 on a carbonaceous surface: a quantum chemical study. *MNRAS*, 384 (3):1158–1164, March 2008. https://doi.org/10.1111/j.1365-2966.2007.12788.x.

Oliver Gressel, Richard P. Nelson, and Neal J. Turner. Dead zones as safe havens for planetesimals: influence of disc mass and external magnetic field. *MNRAS*, 422(2):1140–1159, May 2012. https://doi.org/10.1111/j.1365-2966.2012.20701.x.

Viviana V. Guzmán, Jennifer B. Bergner, Charles J. Law, Karin I. Öberg, Catherine Walsh, Gianni Cataldi, Yuri Aikawa, Edwin A. Bergin, Ian Czekala, Jane Huang, Sean M. Andrews, Ryan A. Loomis, Ke Zhang, Romane Le Gal, Felipe Alarcón, John D. Ilee, Richard Teague, L. Ilsedore Cleeves, David J. Wilner, Feng Long, Kamber R. Schwarz, Arthur D. Bosman, Laura M. Pérez, François Ménard, and Yao Liu. Molecules with ALMA at Planet-forming Scales (MAPS). VI. Distribution of the Small Organics HCN, C_2H, and H_2CO. *ApJS*, 257(1):6, November 2021. https://doi.org/10.3847/1538-4365/ac1440.

Jr. Haisch, Karl E., Elizabeth A. Lada, and Charles J. Lada. Disk Frequencies and Lifetimes in Young Clusters. *ApJL*, 553(2):L153–L156, June 2001. https://doi.org/10.1086/320685.

T. J. Harries, J. D. Monnier, N. H. Symington, and R. K̂urosawa. Three-dimensional dust radiative-transfer models: the Pinwheel Nebula of WR 104. *mnras*, 350:565–574, May 2004. https://doi.org/10.1111/j.1365-2966.2004.07668.x.

T. J. Harries, T. J. Haworth, D. Acreman, A. Ali, and T. Douglas. The TORUS radiation transfer code. *Astronomy and Computing*, 27:63, April 2019. https://doi.org/10.1016/j.ascom.2019.03.002.

Tatsuhiko I. Hasegawa, Eric Herbst, and Chun M. Leung. Models of Gas-Grain Chemistry in Dense Interstellar Clouds with Complex Organic Molecules. *ApJS*, 82:167, September 1992. https://doi.org/10.1086/191713.

John F. Hawley and James M. Stone. Nonlinear Evolution of the Magnetorotational Instability in Ion-Neutral Disks. *ApJ*, 501(2): 758–771, July 1998. https://doi.org/10.1086/305849.

T. Henning and R. Stognienko. Dust opacities for protoplanetary accretion disks: influence of dust aggregates. *A&A*, 311:291–303, July 1996.

Jane Huang, Sean M. Andrews, L. Ilsedore Cleeves, Karin I. Öberg, David J. Wilner, Xuening Bai, Til Birnstiel, John Carpenter, A. Meredith Hughes, Andrea Isella, Laura M. Pérez, Luca Ricci, and Zhaohuan Zhu. CO and Dust Properties in the TW Hya Disk from High-resolution ALMA Observations. *ApJ*, 852(2):122, January 2018. https://doi.org/10.3847/1538-4357/aaa1e7.

John D. Ilee, Catherine Walsh, Alice S. Booth, Yuri Aikawa, Sean M. Andrews, Jaehan Bae, Edwin A. Bergin, Jennifer B. Bergner, Arthur D. Bosman, Gianni Cataldi, L. Ilsedore Cleeves, Ian Czekala, Viviana V. Guzmán, Jane Huang, Charles J. Law, Romane Le Gal, Ryan A. Loomis, François Ménard, Hideko Nomura, Karin I. Öberg, Chunhua Qi, Kamber R. Schwarz, Richard Teague, Takashi Tsukagoshi, David J. Wilner, Yoshihide Yamato, and Ke Zhang. Molecules with ALMA at Planet-forming Scales (MAPS). IX. Distribution and Properties of the Large Organic Molecules HC_3N, CH_3CN, and c-C_3H_2. *ApJS*, 257(1):9, November 2021. https://doi.org/10.3847/1538-4365/ac1441.

S. Ioppolo, H. M. Cuppen, C. Romanzin, E. F. van Dishoeck, and H. Linnartz. Laboratory Evidence for Efficient Water Formation in Interstellar Ices. *ApJ*, 686(2):1474–1479, October 2008. https://doi.org/10.1086/591506.

S. Ioppolo, H. M. Cuppen, C. Romanzin, E. F. van Dishoeck, and H. Linnartz. Water formation at low temperatures by surface O_2 hydrogenation I: characterization of ice penetration. *Physical Chemistry Chemical Physics (Incorporating Faraday Transactions)*, 12(38):12065, January 2010. https://doi.org/10.1039/C0CP00250J.

Andrea Isella, Jane Huang, Sean M. Andrews, Cornelis P. Dullemond, Tilman Birnstiel, Shangjia Zhang, Zhaohuan Zhu, Viviana V. Guzmán, Laura M. Pérez, Xue-Ning Bai, Myriam Benisty, John M. Carpenter, Luca Ricci, and David J. Wilner. The Disk Substructures at High Angular Resolution Project (DSHARP). IX. A High-definition Study of the HD 163296 Planet-forming Disk. *ApJL*, 869(2): L49, December 2018. https://doi.org/10.3847/2041-8213/aaf747.

Anders Johansen and Michiel Lambrechts. Forming Planets via Pebble Accretion. *Annual Review of Earth and Planetary Sciences*, 45(1):359–387, August 2017. https://doi.org/10.1146/annurev-earth-063016-020226.

Joel H. Kastner, C. Qi, D. A. Dickson-Vandervelde, P. Hily-Blant, T. Forveille, S. Andrews, U. Gorti, K. Öberg, and D. Wilner. A Subarcsecond ALMA Molecular Line Imaging Survey of the Circumbinary, Protoplanetary Disk Orbiting V4046 Sgr. *ApJ*, 863(1):106, August 2018. https://doi.org/10.3847/1538-4357/aacff7.

Sebastiaan Krijt, Kamber R. Schwarz, Edwin A. Bergin, and Fred J. Ciesla. Transport of CO in Protoplanetary Disks: Consequences of Pebble Formation, Settling, and Radial Drift. *ApJ*, 864(1):78, September 2018. https://doi.org/10.3847/1538-4357/aad69b.

M. Lambrechts, A. Johansen, and A. Morbidelli. Separating gas-giant and ice-giant planets by halting pebble accretion. *A&A*, 572:A35, December 2014. https://doi.org/10.1051/0004-6361/201423814.

Charles J. Law, Ryan A. Loomis, Richard Teague, Karin I. Öberg, Ian Czekala, Sean M. Andrews, Jane Huang, Yuri Aikawa, Felipe Alarcón, Jaehan Bae, Edwin A. Bergin, Jennifer B. Bergner, Yann Boehler, Alice S. Booth, Arthur D. Bosman, Jenny K. Calahan, Gianni Cataldi, L. Ilsedore Cleeves, Kenji Furuya, Viviana V. Guzmán, John D. Ilee, Romane Le Gal, Yao Liu, Feng Long, François Ménard, Hideko Nomura, Chunhua Qi, Kamber R. Schwarz, Anibal Sierra, Takashi Tsukagoshi, Yoshihide Yamato, Merel L. R. van't Hoff, Catherine Walsh, David J. Wilner, and Ke Zhang. Molecules with ALMA at Planet-forming Scales (MAPS). III. Characteristics of Radial Chemical Substructures. *ApJS*, 257(1):3, November 2021a. https://doi.org/10.3847/1538-4365/ac1434.

Charles J. Law, Richard Teague, Ryan A. Loomis, Jaehan Bae, Karin I. Öberg, Ian Czekala, Sean M. Andrews, Yuri Aikawa, Felipe Alarcón, Edwin A. Bergin, Jennifer B. Bergner, Alice S. Booth, Arthur D. Bosman, Jenny K. Calahan, Gianni Cataldi, L. Ilsedore Cleeves, Kenji Furuya, Viviana V. Guzmán, Jane Huang, John D. Ilee, Romane Le Gal, Yao Liu, Feng Long, François Ménard, Hideko Nomura, Laura M. Pérez, Chunhua Qi, Kamber R. Schwarz, Daniela Soto, Takashi Tsukagoshi, Yoshihide Yamato, Merel L. R. van't Hoff, Catherine Walsh, David J. Wilner, and Ke Zhang. Molecules with ALMA at Planet-forming Scales (MAPS). IV. Emission Surfaces and Vertical Distribution of Molecules. *ApJS*, 257 (1):4, November 2021b. https://doi.org/10.3847/1538-4365/ac1439.

Romane Le Gal, Madison T. Brady, Karin I. Öberg, Evelyne Roueff, and Franck Le Petit. The Role of C/O in Nitrile Astrochemistry in PDRs and Planet-forming Disks. *ApJ*, 886(2):86, December 2019. https://doi.org/10.3847/1538-4357/ab4ad9.

Ryan A. Loomis, L. Ilsedore Cleeves, Karin I. Öberg, Yuri Aikawa, Jennifer Bergner, Kenji Furuya, V. V. Guzman, and Catherine Walsh. The Distribution and Excitation of CH_3CN in a Solar Nebula Analog. *ApJ*, 859(2):131, June 2018. https://doi.org/10.3847/1538-4357/aac169.

L. B. Lucy. Computing radiative equilibria with Monte Carlo techniques. *A&A*, 344:282–288, April 1999.

D. Lynden-Bell and J. E. Pringle. The evolution of viscous discs and the origin of the nebular variables. *MNRAS*, 168: 603–637, Sep 1974. https://doi.org/10.1093/mnras/168.3.603.

J. S. Mathis, W. Rumpl, and K. H. Nordsieck. The size distribution of interstellar grains. *ApJ*, 217:425–433, October 1977. https://doi.org/10.1086/155591.

D. McElroy, C. Walsh, A. J. Markwick, M. A. Cordiner, K. Smith, and T. J. Millar. The UMIST database for astrochemistry 2012. *A&A*, 550:A36, February 2013. https://doi.org/10.1051/0004-6361/201220465.

J. P. McMullin, B. Waters, D. Schiebel, W. Young, and K. Golap. CASA Architecture and Applications. In R. A. Shaw, F. Hill, and D. J. Bell, editors, *Astronomical Data Analysis Software and Systems XVI*, volume 376 of *Astronomical Society of the Pacific Conference Series*, page 127, October 2007.

A. Miotello, S. Facchini, E. F. van Dishoeck, P. Cazzoletti, L. Testi, J. P. Williams, M. Ansdell, S. van Terwisga, and N. van der Marel. Bright C_2H emission in protoplanetary discs in Lupus: high volatile C/O > 1 ratios. *A&A*, 631:A69, November 2019. https://doi.org/10.1051/0004-6361/201935441.

A. Miotello, I. Kamp, T. Birnstiel, L. I. Cleeves, and A. Kataoka. Setting the Stage for Planet Formation: Measurements and Implications of the Fundamental Disk Properties. *arXiv e-prints*, art. arXiv:2203.09818, March 2022.

H. S. P. Müller, S. Thorwirth, D. A. Roth, and G. Winnewisser. The Cologne Database for Molecular Spectroscopy, CDMS. *A&A*, 370:L49–L52, April 2001. https://doi.org/10.1051/0004-6361:20010367.

Holger S. P. Müller, Frank Schlöder, Jürgen Stutzki, and Gisbert Winnewisser. The Cologne Database for Molecular Spectroscopy, CDMS: a useful tool for astronomers and spectroscopists. *Journal of Molecular Structure*, 742(1-3):215–227, May 2005. https://doi.org/10.1016/j.molstruc.2005.01.027.

Joan R. Najita, Máté Ádámkovics, and Alfred E. Glassgold. Formation of Organic Molecules and Water in Warm Disk Atmospheres. *ApJ*, 743(2):147, December 2011. https://doi.org/10.1088/0004-637X/743/2/147.

Y. Oba, N. Watanabe, T. Hama, K. Kuwahata, H. Hidaka, and A. Kouchi. Water Formation through a Quantum Tunneling Surface Reaction, OH + H_2, at 10 K. *ApJ*, 749(1):67, April 2012. https://doi.org/10.1088/0004-637X/749/1/67.

Karin I. Öberg, A. C. Adwin Boogert, Klaus M. Pontoppidan, Saskia van den Broek, Ewine F. van Dishoeck, Sandrine Bottinelli, Geoffrey A. Blake, and II Evans, Neal J. The Spitzer Ice Legacy: Ice Evolution from Cores to Protostars. *ApJ*, 740(2):109, October 2011. https://doi.org/10.1088/0004-637X/740/2/109.

Karin I. Öberg, Viviana V. Guzmán, Kenji Furuya, Chunhua Qi, Yuri Aikawa, Sean M. Andrews, Ryan Loomis, and David J. Wilner. The comet-like composition of a protoplanetary disk as revealed by complex cyanides. *Nature*, 520(7546): 198–201, April 2015. https://doi.org/10.1038/nature14276.

Karin I. Öberg, Viviana V. Guzmán, Catherine Walsh, Yuri Aikawa, Edwin A. Bergin, Charles J. Law, Ryan A. Loomis, Felipe Alarcón, Sean M. Andrews, Jaehan Bae, Jennifer B. Bergner, Yann Boehler, Alice S. Booth, Arthur D. Bosman, Jenny K. Calahan, Gianni Cataldi, L. Ilsedore Cleeves, Ian Czekala, Kenji Furuya, Jane Huang, John D. Ilee, Nicolas T. Kurtovic, Romane Le Gal, Yao Liu, Feng Long, François Ménard, Hideko Nomura, Laura M. Pérez, Chunhua Qi, Kamber R. Schwarz, Anibal Sierra, Richard Teague, Takashi Tsukagoshi, Yoshihide Yamato, Merel L. R. van't Hoff, Abygail R. Waggoner, David J. Wilner, and Ke Zhang. Molecules with ALMA at Planet-forming Scales (MAPS). I. Program Overview and Highlights. *ApJS*, 257(1):1, November 2021. https://doi.org/10.3847/1538-4365/ac1432.

Daniel Perez-Becker and Eugene Chiang. Surface Layer Accretion in Conventional and Transitional Disks Driven by Far-ultraviolet Ionization. *ApJ*, 735(1):8, July 2011. https://doi.org/10.1088/0004-637X/735/1/8.

Matthew W. Powner, Béatrice Gerland, and John D. Sutherland. Synthesis of activated pyrimidine ribonucleotides in prebiotically plausible conditions. *Nature*, 459(7244):239–242, May 2009. https://doi.org/10.1038/nature08013.

Dougal Ritson and John D. Sutherland. Prebiotic synthesis of simple sugars by photoredox systems chemistry. *Nature Chemistry*, 4(11):895–899, November 2012. https://doi.org/10.1038/nchem.1467.

Deborah P. Ruffle and Eric Herbst. New models of interstellar gas-grain chemistry - III. Solid CO_2. *MNRAS*, 324(4):1054–1062, July 2001. https://doi.org/10.1046/j.1365-8711.2001.04394.x.

F. L. Schöier, F. F. S. van der Tak, E. F. van Dishoeck, and J. H. Black. An atomic and molecular database for analysis of submillimetre line observations. *A&A*, 432(1):369–379, March 2005. https://doi.org/10.1051/0004-6361:20041729.

Kamber R. Schwarz, Edwin A. Bergin, L. Ilsedore Cleeves, Ke Zhang, Karin I. Öberg, Geoffrey A. Blake, and Dana Anderson. Unlocking CO Depletion in Protoplanetary Disks. I. The Warm Molecular Layer. *ApJ*, 856(1):85, March 2018. https://doi.org/10.3847/1538-4357/aaae08.

John D. Sutherland. The Origin of Life - Out of the Blue. *Angewandte Chemie*, 55(1):104–121, October 2015. https://doi.org/10.1002/anie.201506585.

Richard Teague. Gofish: Fishing for line observations in protoplanetary disks. *The Journal of Open Source Software*, 4 (41):1632, sep 2019. https://doi.org/10.21105/joss.01632. URL https://doi.org/10.21105/joss.01632.

Richard Teague, Jaehan Bae, and Edwin A. Bergin. Meridional flows in the disk around a young star. *Nature*, 574(7778):378–381, October 2019. https://doi.org/10.1038/s41586-019-1642-0.

W. F. Thi, G. Mathews, F. Ménard, P. Woitke, G. Meeus, P. Riviere-Marichalar, C. Pinte, C. D. Howard, A. Roberge, G. Sandell, I. Pascucci, B. Riaz, C. A. Grady, W. R. F. Dent, I. Kamp, G. Duchêne, J. C. Augereau, E. Pantin, B. Vandenbussche, I. Tilling, J. P. Williams, C. Eiroa, D. Barrado, J. M. Alacid, S. Andrews, D. R. Ardila, G. Aresu, S. Brittain, D. R. Ciardi, W. Danchi, D. Fedele, I. de Gregorio-Monsalvo, A. Heras, N. Huelamo, A. Krivov, J. Lebreton, R. Liseau, C. Martin-Zaidi, I. Mendigutía, B. Montesinos, A. Mora, M. Morales-Calderon, H. Nomura, N. Phillips, L. Podio, D. R. Poelman, S. Ramsay, K. Rice, E. Solano, H. Walker, G. J. White, and G. Wright. Herschel-PACS observation of the 10 Myr old T Tauri disk TW Hya. Constraining the disk gas mass. *A&A*, 518:L125, July 2010. https://doi.org/10.1051/0004-6361/201014578.

Eric Van Clepper, Jennifer B. Bergner, Arthur D. Bosman, Edwin Bergin, and Fred J. Ciesla. Chemical Feedback of Pebble Growth: Impacts on CO depletion and C/O ratios. *ApJ*, 927(2): 206, March 2022. https://doi.org/10.3847/1538-4357/ac511b.

A. I. Vasyunin and Eric Herbst. Reactive Desorption and Radiative Association as Possible Drivers of Complex Molecule Formation in the Cold Interstellar Medium. *ApJ*, 769(1):34, May 2013. https://doi.org/10.1088/0004-637X/769/1/34.

Catherine Walsh, Tom. J. Millar, Hideko Nomura, Eric Herbst, Susanna Widicus Weaver, Yuri Aikawa, Jacob C. Laas, and Anton I. Vasyunin. Complex organic molecules in protoplanetary disks. *A&A*, 563:A33, March 2014. https://doi.org/10.1051/0004-

Stephen G. Warren and Richard E. Brandt. Optical constants of ice from the ultraviolet to the microwave: A revised compilation. *Journal of Geophysical Research (Atmospheres)*, 113(D14):D14220, July 2008. https://doi.org/10.1029/2007JD009744.

P. Woitke, I. Kamp, and W. F. Thi. Radiation thermo-chemical models of protoplanetary disks. I. Hydrostatic disk structure and inner rim. *A&A*, 501(1):383–406, July 2009. https://doi.org/10.1051/0004-6361/200911821.

C. Xie, S. Y. Haffert, J. de Boer, M. A. Kenworthy, J. Brinchmann, J. Girard, I. A. G. Snellen, and C. U. Keller. A MUSE view of the asymmetric jet from HD 163296. *A&A*, 650:L6, June 2021. https://doi.org/10.1051/0004-6361/202140602.

Ke Zhang, Alice S. Booth, Charles J. Law, Arthur D. Bosman, Kamber R. Schwarz, Edwin A. Bergin, Karin I. Öberg, Sean M. Andrews, Viviana V. Guzmán, Catherine Walsh, Chunhua Qi, Merel L. R. van't Hoff, Feng Long, David J. Wilner, Jane Huang, Ian Czekala, John D. Ilee, Gianni Cataldi, Jennifer B. Bergner, Yuri Aikawa, Richard Teague, Jaehan Bae, Ryan A. Loomis, Jenny K. Calahan, Felipe Alarcón, François Ménard, Romane Le Gal, Anibal Sierra, Yoshihide Yamato, Hideko Nomura, Takashi Tsukagoshi, Laura M. Pérez, Leon Trapman, Yao Liu, and Kenji Furuya. Molecules with ALMA at Planet-forming Scales (MAPS). V. CO Gas Distributions. *ApJS*, 257(1):5, November 2021. https://doi.org/10.3847/1538-4365/ac1580.